AD-A065 009 SPECTROLAB INC SYLMAR CALIF F/G 10/2

HIGH EFFICIENCY SOLAR PANEL (HESP-II).(U)

AUG 78 P M STELLA, F M UNO, J W THORNHILL F33615-77-C-3108

UNCLASSIFIED AFAPL-TR-78-60 NL

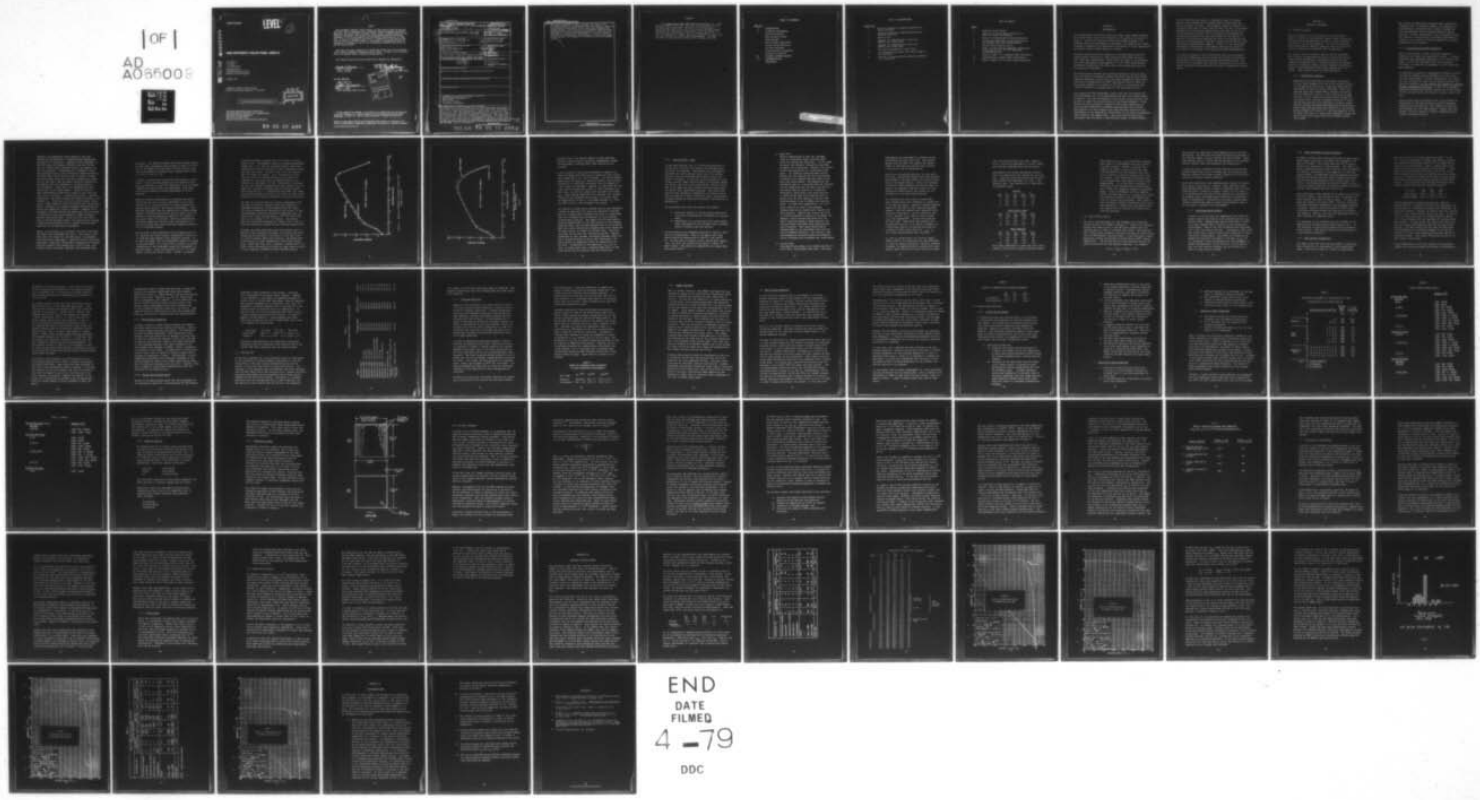

END

DATE FILMED

4 -79

DDC

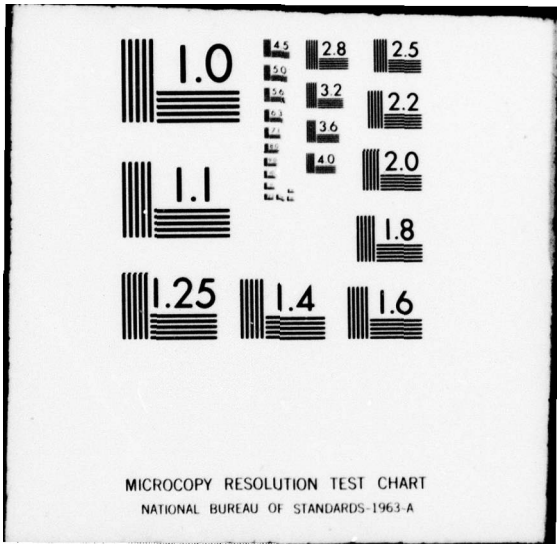
1.0
1.1
1.25
1.4
1.6
1.8
2.0
2.2
2.5
2.8
3.2
3.6
4.0
4.5
5.0
MICROCOPY RESOLUTION TEST CHART
NATIONAL BUREAU OF STANDARDS-1963-A

AFAPL-TR-78-60

LEVEL II

(2)

HIGH EFFICIENCY SOLAR PANEL (HESP-II)

P. M. STELLA
F. M. UNO
J. W. THORNHILL

SPECTROLAB, INC.
12500 GLADSTONE AVENUE
SYLMAR, CALIFORNIA 91342

AUGUST 1978

TECHNICAL REPORT AFAPL-TR-78-60
Interim Technical Report August 1977 – June 1978

Approved for public release; distribution unlimited.

AIR FORCE AERO PROPULSION LABORATORY
AIR FORCE WRIGHT AERONAUTICAL LABORATORIES
AIR FORCE SYSTEMS COMMAND
UNITED STATES AIR FORCE
WRIGHT-PATTERSON AIR FORCE BASE, OHIO 45433

NOTICE

When Government drawings, specifications, or other data are used for any purpose other than in connection with a definitely related Government procurement operation, the United States Government thereby incurs no responsibility nor any obligation whatsoever; and the fact that the government may have formulated, furnished, or in any way supplied the said drawings, specifications, or other data, is not to be regarded by implication or otherwise as in any manner licensing the holder or any other person or corporation, or conveying any rights or permission to manufacture, use, or sell any patented invention that may in any way be related thereto.

This report has been reviewed by the Information Office (OI) and is releasable to the National Technical Information Service (NTIS). At NTIS, it will be available to the general public, including foreign nations.

This technical report has been reviewed and is approved for publication.

Lowell D. Massie
LOWELL D. MASSIE
Project Engineer

R.R. Barthelemy
R.R. BARTHELEMY
Chief, Energy Conversion Branch

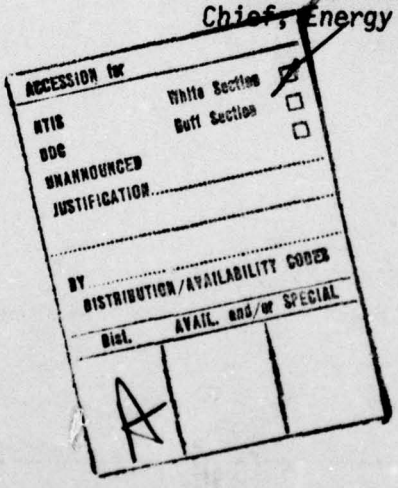

FOR THE COMMANDER

JAMES D. REAMS
Chief, Aerospace Power Division

"If your address has changed, if you wish to be removed from our mailing list, or if the addressee is no longer employed by your organization please notify AFAPL/POE *, W-PAFB, OH 45433 to help us maintain a current mailing list".*

Copies of this report should not be returned unless return is required by security considerations, contractual obligations, or notice on a specific document.

AIR FORCE/56780/21 February 1979 — 210

UNCLASSIFIED

SECURITY CLASSIFICATION OF THIS PAGE (When Data Entered)

REPORT DOCUMENTATION PAGE

READ INSTRUCTIONS BEFORE COMPLETING FORM

1. REPORT NUMBER: AFAPL-TR-78-60	2. GOVT ACCESSION NO.
3. RECIPIENT'S CATALOG NUMBER: Final	
4. TITLE (and Subtitle): HIGH EFFICIENCY SOLAR PANEL (HESP-II).	5. TYPE OF REPORT & PERIOD COVERED: Interim Technical Report. Aug 1977-Jun 1978
	6. PERFORMING ORG. REPORT NUMBER
7. AUTHOR(s): P. M. Stella, F. M. Uno, and J. W. Thornhill	8. CONTRACT OR GRANT NUMBER(s): F33615-77-C-3108
9. PERFORMING ORGANIZATION NAME AND ADDRESS: Spectrolab, Inc. 12500 Gladstone Avenue Sylmar, CA. 91342	10. PROGRAM ELEMENT, PROJECT, TASK AREA & WORK UNIT NUMBERS: 682J2404-05
11. CONTROLLING OFFICE NAME AND ADDRESS: Air Force Aero Propulsion Laboratory/POE-2 Air Force Wright Aeronautical Laboratories (AFSC) Wright-Patterson Air Force Base, OH 45433	12. REPORT DATE: August 1978
	13. NUMBER OF PAGES: 74p.
14. MONITORING AGENCY NAME & ADDRESS (if different from Controlling Office)	15. SECURITY CLASS. (of this report): Unclassified
	15a. DECLASSIFICATION DOWNGRADING SCHEDULE

16. DISTRIBUTION STATEMENT (of this Report)

Approved for public release; distribution unlimited.

17. DISTRIBUTION STATEMENT (of the abstract entered in Block 20, if different from Report)

18. SUPPLEMENTARY NOTES

19. KEY WORDS (Continue on reverse side if necessary and identify by block number)

Advanced silicon solar cells
Solar energy conversion
Space Power
Radiation effects
Si surface treatments

20. ABSTRACT (Continue on reverse side if necessary and identify by block number)

The objective of this program is to develop space qualified weapon survivable silicon solar cells having a BOL conversion efficiency of 16% at 25 C under AMO illumination. After seven (7) years in the synchronous orbit environment (approximately 3 x 10 exp. (14) 1 meV electrons/square centimeter equivalent irradiation) the cells shall not degrade more than 13% in conversion efficiency. The status of the work at this point and the performance of the most recent state-of-the-art cells delivered as representative samples are reported.

→ next Page

DD FORM 1 JAN 73 1473 EDITION OF 1 NOV 65 IS OBSOLETE

UNCLASSIFIED

SECURITY CLASSIFICATION OF THIS PAGE (When Data Entered)

20. The results obtained to date indicate that some of the processes chosen for optimization have not proven as fruitful as originally anticipated, while others have demonstrated marked success. The task now is to integrate these various optimizations into an integrated sequence to fabricate cells that meet or surpass the requirements. A list of possible additional investigations, which appear pertinent and useful to this effort, is included in the section entitled Recommendations.

FOREWORD

This final report was submitted by Spectrolab, Inc. under contract F33615-77-C-3108. The effort was sponsored by the Air Force Aero Propulsion Laboratory, Air Force Wright Aeronautical Laboratories, Air Force Systems Command, Wright-Patterson AFB, Ohio under Project 682J, Task No. 682J04 and Work Unit No. 682J0405 with Lowell D. Massie (POE-2) as Project Engineer in charge. Mr Jay W. Thornhill of Spectrolab, Inc. was technically responsible for the work. The work covered the time period of August 1977 through June 1978.

TABLE OF CONTENTS

LIST OF ILLUSTRATIONS

LIST OF TABLES

SECTION I

INTRODUCTION

This second phase of the High Efficiency Solar Panel (HESP) program for silicon solar cells is an extension of the efforts and goals of Phase I. During this portion of the overall HESP program it is intended that cell development be completed, thus permitting a demonstration of advanced cell production, the design of flight experiments, and finally actual flight testing to follow.

The main objective of this program is to develop space qualified silicon solar cells having a BOL conversion efficiency of 16% at $25^{o}C$ under AMO illumination. After seven (7) years in the synchronous orbit environment (approximately 3×10^{14} 1 MeV electrons/cm^2 equivalent irradiation) the cells shall not degrade more than 13% in conversion efficiency.

The metallization systems and coverglass adhesives are to be such that the cells can withstand thermal excursions and cycling without adhesive debonding or more than a 20% power degradation after being subjected to temperatures of $260^{o}C$ for sixteen hours or $400^{o}C$ for one hundred seconds in a vacuum of 10^{-5} Torr, or 500 cycles from $-160^{o}C$ to $+100^{o}C$ at a minimum rate of $30^{o}C$ per minute in air.

The program has been organized in such a way that the process and cell development are to be completed during the first twelve months of effort. The last two months of this period include process integration to permit the finalization of the process sequence. Three months are then provided to accomplish the actual fabrication of the cells and demonstration modules required under the contract. Three months are then occupied with qualification testing and the measurement of the temperature coefficients of the cells to establish their behavior and capabilities. The cells must be qualified in accordance with the Table I "Qualification Tests" of MIL-C-83443A.

This Interim Technical Report is intended to show the current status of the program and the progress made to date after the first ten months of effort. The Technical Discussion section of the report describes in detail the work done this far on the various segments of the processing sequence and gives some insight as to the thinking and rationale used in developing the processes and techniques for meeting the cell requirements of the contract. A section is included that describes the status of the work at this point and the performance of the most recent state-of-the-art cells delivered as representative samples. Finally, a list of possible additional investigations, which appear pertinent and useful to this effort, is included in the section entitled Recommendations.

The results obtained to date indicate that some of the processes chosen for optimization have not proven as fruitful as originally anticipated, while others have demonstrated marked success. The task now is to integrate these various optimizations into an integrated sequence to fabricate cells that meet or surpass the requirements.

SECTION II

TECHNICAL DISCUSSION

2.1 Surface Treatment

Surface treatment, for the purposes of this discussion, does not include the conventional damage removal etching and surface texturizing performed initially on silicon blanks at the start of the process sequence. Here surface treatment means those special chemical operations used to prepare the silicon surface for a subsequent step or operation.

The initial intent in applying special surface treatments was to remove contaminants from the silicon which might provide a source for material contamination during the high temperature diffusion step. This was modified and expanded during the program to include surface treatments during other phases of cell fabrication which might improve final cell output. These separate areas are discussed below.

2.1.1 Prediffusion Cleaning

Experiments were performed to investigate the removal of heavy metal elements from the silicon surface following the hydroxide etch cycles, since such materials are detrimental to minority carrier lifetimes. Cells were prepared using the standard HESP-I process varying only the post NaOH etch cleaning. These variations included DI water rinsing, hydrochloric acid soaking followed by a DI water rinse, soaking in peroxide solutions of hydrochloric and sulphuric acids followed by DI water rinses, and PNH cleaning (peroxide-ammonium-hydroxide-hydrochloric acid), which had been found very effective in precleaning boron diffused P-on-N cells.[1] With the exception of the DI water rinse only, all groups were essentially identical; the DI water rinse group exhibiting a slightly poorer curve shape.

The results of these tests indicated that surface pretreatment prior to diffusion appears to be adequate if a hydrochloric acid-water soak is used to remove the iron contamination from the sodium hydroxide etched surfaces. Further pretreatment, such as peroxide cleaning, offers no statistically significant improvement in current or fill factor as might be expected if residual contamination were present.

2.1.2 Precontacting Surface Treatments

During this program a surface treatment capable of improving cell output was examinted in detail. Although differing from approaches suggested in the contract proposal, in that the treatment occurs after junction diffusion, a significant improvement in cell output has been observed.

An exploratory sequence of experiments indicated a strong correlation between surface treatment prior to contacting and improvements in output currents and fill factor. The use of dilute HF, which is the standard surface preparation technique, may be harmful with respect to reducing surface recombination velocity. A test lot of ammonium hydroxide treated wafers proved superior to an HF treated control group by nearly two percent in short circuit current.

These results were so promising that it was decided to concentrate on the post diffusion surface treatments, rathern then pre-diffusion. This implied an entirely new mechanism for cell improvements. Rather than bulk effects, we were looking at surface recombination and contact resistance effects.

Normally the phosphorous oxide formed on the cell surface during diffusion is removed using hydrofluoric acid prior to contacting. Because of this treatment it was felt that the residual fluoride ions left on the silicon surface might adversely affect the behavior of the cell contacts. Consequentially a number of cells were prepared using a low concentration ammonium hydroxide soak after the HF step in order to leave a "clean" silicon surface (plus the usual thin oxides which might form in the short time the wafers would be subjected to the ambient prior to placement in the metallization vacuum system). These were to be compared with cells fabricated in the normal manner. Electrical performance measurements showed both groups to have identical open circuit voltages, a disappointing result. However, unexpectedly the group treated with NH_4OH exhibited a 2.5% greater I_{sc}. Since the cells were not AR coated, variations in that operation would not account for the discrepancy. Inspection of contact coverage indicated that all cells were essentially equally covered. Inasmuch as no processing variation beyond the NH_4OH step could be found, an additional group was processed in order to obtain a greater statistical base. Since the first test group used 10 ohm-cm polished wafers, the second group utilized 2 ohm-cm textured wafers since 2 ohm-cm cells are more sensitive to the fabrication processes.

Again, no significant V_{oc} difference was noted (although the NH_4OH group averaged 0.4% lower). The current, however, was 1.5% higher for the same group, in agreement with the earlier experiment. Since the current variations were small, additional groups were processed with varying diffusion depths, bulk resistivity (2 and 10 ohm), and surface finish (polished, textured, and hydroxide semi-

polished). The NH_4OH processed cells were always higher, so that after processing seven groups of cells (117 cells total) the NH_4OH cells averaged 2.5% more current than the conventionally processed cells, ranging from a high of 3.3% to a low of 1.5%.

A number of additional findings were determined in these tests. First, the enhancement was also observed after Ta_2O_5 AR coating, so that the possibility of a thin NH_4OH induced AR coating effect was eliminated. With about 60 cells AR coated an average improvement of 2% was measured.

Spectral response measurements of uncoated and coated cells show the gain to occur essentially at all wavelengths up to .95 microns with a slightly greater percentage gain evident at the shorter wavelengths. This behavior indicated that the possibility of higher output because of junction etching was not the case, since the impact of junction shallowing typically is limited to the region below 0.75 microns. This was independently checked by measuring junction sheet resistance with a four point probe both before and after NH_4OH processing, with no indicated change.

At this time it was postulated that the NH_4OH might be (1) reducing the front surface recombination velocity or (2) removing some unknown light absorbing residue. If it were the former then the enhancement should be related to junction depth. If it were due to removal of surface contamination, the enhancement syould be independent of junction depth. Cells were examined for ρ_s = 210 ohms/square, along with control cells. Indeed, the deeper

diffusions showed a greater gain (3.3%) than the shallower (2.3%). Furthermore, spectral response measurements showed that if it were not for some atypical long wavelength gains inthe shallow cells, their enhancement would have been even less. Figures 1 and 2 give the spectral data for these two groups. It is interesting to note that even the very shallow diffusion cells gained in response at .4 microns from the NH_4OH process by the relatively large amount of 5.9%. Additionally, although all the very shallow diffused cells were limited in curve shape due to series resnstance (grid structures which were optimized for ρs = ohms/square were used) the higher blue response NH_4OH cells were 5.1% higher at load, inconsistent with any remaining thoughts of junction thinning.

The data on junction depth and current enhancement from the deep and shallow junction tests were compared to published theoretical curves demonstrating the impact of surface recombination velocity on cell output (2) and some agreement could be obtained by suggesting that the initial cell front surface has $S_F = 10^5 - 10^6$ cm/sec and that it was reduced to $10^2 - 10^3$ cm/sec. Such values have been previously measured for typical solar cell surfaces and specially cleaned silicon surfaces respectively.

Although the cells described above were treated prior to Ag-Pd-Ti rear contacting (followed by sintering and front contacting with Ag-Pd-Ti or Ag-Pd-Ta) it was felt that if a front surface effect was occurring, the NH_4OH could be done prior to front contacting or even after contacting. Tests here show that in general, cleaning prior to front contact application provides the same result as prior to rear contacts, although a slight variance exists,

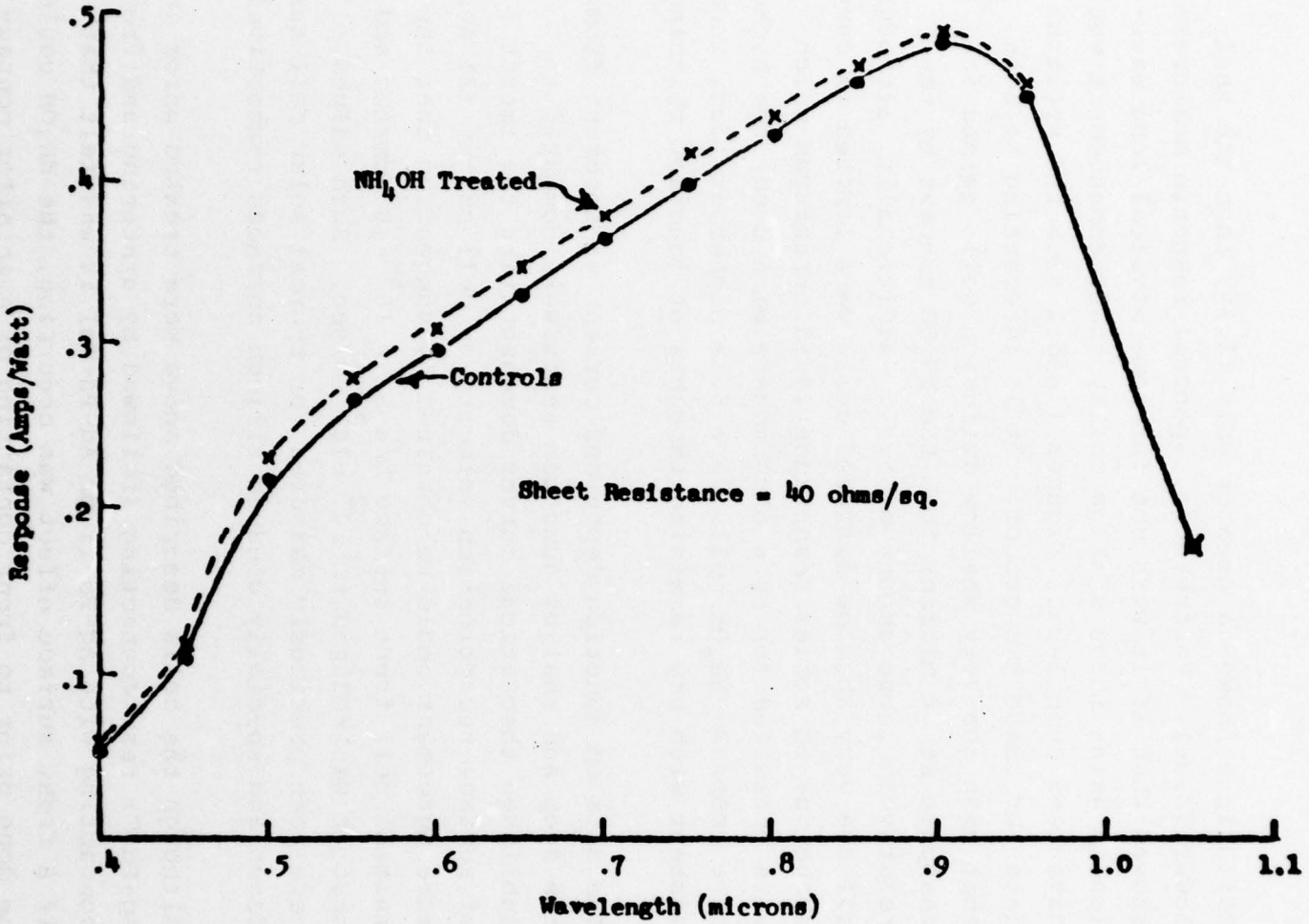

Figure 1. Spectral Response of NH_4OH Treated Cells
(Deep Junction)

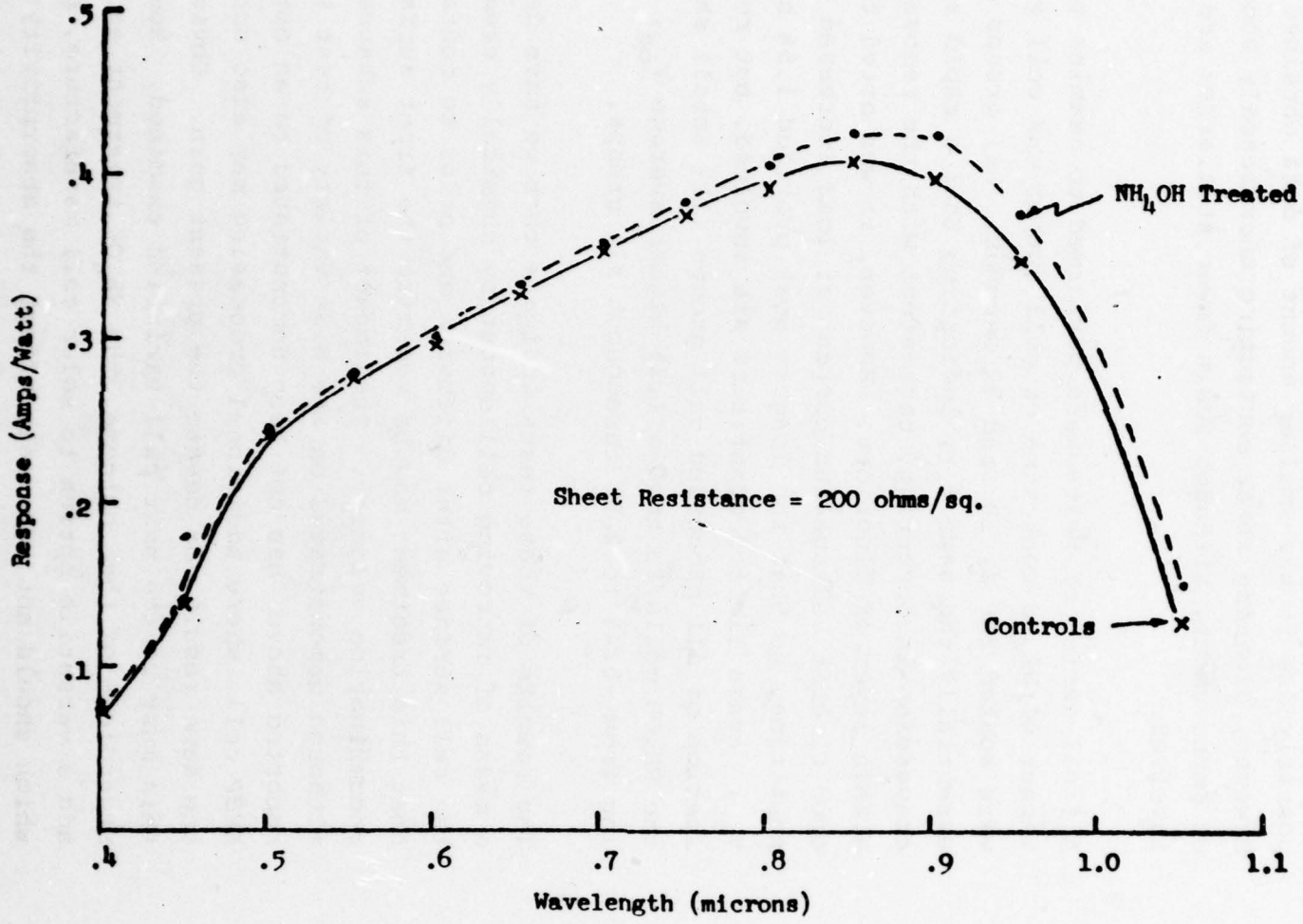

Spectral Response of NH_4OH Treated Cells
(Shallow Junction)

Figure 2

possibly due to the smaller amount of data obtained. However, cleaning after contacting unexpectedly showed no improvement, although again fewer statistics are involved.

A final series of tests were performed to examine the impact of NH_4OH soak time on cell output and cell groups were soaked for 2, 10, and 30 seconds. All groups showed essentially the same I_{sc}, indicating that a rapid surface conversion is occurring, consistent with the removal of a thin layer of fluorides. However, it was noted that the open circuit voltage and current at load increased with soak time, so that the longest soak provided 1.5% higher V_{oc}. Again limited quantities are involved, but re-examination of all processed cell groups (117 total) shows the NH_4OH cells to have a 1.2% higher average V_{oc}, varying from -0.4% to 2.8% throughout all groups.

The results of these tests indicate that we have developed a means of improving cell output by chemically treating the cell surface after diffusion and prior to contacting; that this treatment may be reducing the front surface recombination velocity. The impact of this enhancement, although demonstrated on the wide variety of test samples reported above, has not been demonstrated on an optimized HESP cell, where additional processing may also accomplish the same result, or negate the present gain. Obviously this must be the next cell variation examined. However, regardless of that outcome, the NH_4OH treatment above can add a versatile option to solar cell manufacture, one which should not adversely effect the absorptivity of the cell. Furthermore if the additional V_{oc} gain is real, it would imply that a combined power gain of over four percent may be possible with this technique.

2.1.3 Junction Etch - Back

It had been observed that if a Ti-Pd metallization is etched from a silicon cell surface the diffused layer thickness is decreased. Experiments were performed to determine why this occurred and to see if an etching solution could be developed which would control the amount of etching. It was felt to be desirable to have a deep junction under the grid metal to eliminate spikes and shorts, which can occur with shallow junction cells, and at the same time have shallow junction active areas for better short wavelength response. This would also improve laser hardening, weldability, AR coating treatment variability, overall electrical yield, and possibly increase voltage by reducing the surface concentration of phosphorous.

Two approaches were taken to achieve this effect:

1) Selective etching of a Ti-Pd coating metallization whith simultaneously decreased the junction depth.
2) Development of a silicon etch that would remove small increments of the diffused layer uniformly, without attacking the grid pattern.

Silicon material was phosphine diffused to obtain a sheet rho of 45 ohms/square. Some of the wafers were then metallized by EB evaporation of 3000 Å Ti and 3000 Å Pd. To show that no reaction occurs during metal deposition, one wafer was etched in hot H_2SO_4 to remove the metal layers. The sheet rho reading did not change from the initial value.

1) Metal Etch

Various combinations of H_2O, HF, and HNO_3 (both a Si and metal etch) solutions were tried for etching the metal pair. In all cases the metal was etched or floated off and some increment of Si dissolved. However, the silicon surface was discolored by a nonuniform oxide layer. V/I readings indicated some silicon removal but the reaction was not controllable. In addition the unmetallized back side of the wafer was being etched. The possibility was considered that Ti in solution with the fluoride ion was responsible for the back side etching. This would then be similar to a technique developed by Spectrolab a few years previous in which HF was used with aluminum metal to slowly etch off thin regions of silicon from diffused wafers so as to reduce the junction depth. To check this possibility, a 3×10^{-2} molar solution of TiF_6^{-2} was prepared. Unmetallized silicon wafers were treated with this solution. Soaking the silicon for up to 17 minutes produced no change in the sheet rho. However, etching metallized cells with the TiF_6^{-2} solution caused a rapid reaction, but the previously mentioned oxide discoloration still occurred. This oxide discoloration problem seems to be unavoidable even with the use of buffered solutions. As a result, this electrochemical etching process was abandoned and an alternate etch treatment was investigated.

2) Silicon Etch

CrO_3:H_2O:HF was chosen as an etchant because it has a slow, controllable etch rate. The first

experiments were performed on diffused silicon to establish an exact etch rate. The results showed that the sheet rho reading was proportional to the etch time and the etch rate was a function of the HF concentration.

Using this CrO_3:H_2O:HF solution, silicon cells with only a titanium-palladium metal grid pattern were etched to see what effect the solution would have on the metallization. After a few seconds of etching, which produced the desired sheet rho reading, no apparent etching of even this thin unprotected metallization was visible in the microscope at low power magnification.

The procedure was then tried on texturized, back surface field cells diffused to a sheet rho of 36 ohms per square. Spectral response measurements were then made on the junction etch-back samples. The test samples were completed cells (without AR coatings). Initial values of open circuit voltage (V_{oc}), short circuit current (I_{sc}) and responsivity (R,A/W) were measured for each cell. Cells were then etched with a CrO_3:H_2O:HF solution in 30 second increments for a total etch time of 150 seconds and baked for 1 minute at 400°C after each etch. V_{oc}, I_{sc} and R were measured after each increment.

V_{oc} and I_{sc} showed gains of 1% and 4% respectively after a 30 second etch and then decreased in value as etching continued. Spectral response, likewise, is improved after 30 seconds etch time. Typical gains were 13% at 400 nm and 6% at 950nm.

After 150 seconds total etch time, responsivity at 400 nm has decreased to initial values, but long wave response still has a 5% gain.'

Measurements from these experiments indicate that a 30 second etch was optimum for cell output. Three new cells were etched (30 seconds), baked (400°C) and submitted to a 65°C, 7 day humidity test. The following is a compilation of measured values.

Initial

Cell No.	V_{oc} (mV)	I_{sc} (mA)	R_{400} (A/W)	R_{950} (A/W)
6	612	131	.08	.78
7	612	135	.09	.80
24	609	133	.08	.81

After Etch & Bake

Cell No.	V_{oc} (mV)	I_{sc} (mA)	R_{400} (A/W)	R_{950} (A/W)
6	617	142	.105	.82
7	614	145	.11	.87
24	615	143	.105	.88

After Humidity

Cell No.	V_{oc} (mV)	I_{sc} (mA)	R_{400} (A/W)	R_{950} (A/W)
6	614	141	.105	.80
7	614	144	.105	.85
24	613	143	.105	.85

Cells were submitted to a tape test (810) after humidity test and all contacts remained intact.

Improvements in V_{oc}, I_{sc} and spectral response were shown to be realizable with the junction etch-back process. However, although such samples had higher current output than deep diffused wafers with the etch-back they were still inferior to shallow diffused cells after AR coating. This difference was greater than any estimated gain from higher AR coating bake temperatures. It is felt that a reduction in efficiency of the nonreflecting surface might be at fault; for example a change in tetrahedral shape. Since tetrahedrons could be observed before and after etching it is likely that higher rate etching occurred at the tetrahedron tips so as to flatten the structures. With sufficient flattening multiple reflections would occur less frequently. Further work was halted since the results did not indicate any overall gain could be realized.

2.2 Back Surface Fields

The use of aluminum paste for BSF formation was introduced toward the end of the HESP-I contract.[3] During this contract efforts were made to see if the BSF paste process could be improved upon in order to increase cell output. One alternate back surface field formation technique utilized the screen printing of aluminothermic reaction pairs. It was felt that a boron doped back surface field might be achievable at 900°C furnace temperature. The driving force of this reaction follows the same principles as for the thermite reaction. For example:

$$2\ Al + In_2O_3 \longrightarrow Al_2O_3 + 2\ In$$

The reaction is initiated at high temperatures and is self-sustaining. The heat from the reaction would be localized in the reaction region, and not through the entire wafer. Using such reaction pairs it would then be possible to try multiple acceptor doping, both simultaneously and sequentially.

It was felt that a successful boron technique could possibly provide higher open circuit voltages and, by localizing the heating, preserve the single crystal integrity of the silicon resulting in better contact stability.

Cells were fabricated using aluminum paste altered to contain B_2O_3, Ga_2O_3, In_2O_3 and In. However, after repeated trials such additions were found to offer no advantage over the usual aluminum paste in terms of voltage, current or fill factor. It is possible that the heat of the reaction was insufficient to provide either increased dopant solubility or increased depth of penetration. Returning to the basic aluminum paste process, efforts were made to refine the procedures then in use in order to optimize cell performance.

2.2.1 Time-Temperature Effects

A matrix of firing times and temperatures was tested to compare current and voltage gains obtained from the back surface field. Temperatures varying from 800°C to 950°C with times ranging from 10 seconds to 120 seconds were investigated. Each of the time increments was subdivided into a fast cool and a slow cool. A minimum of eight cells were fabricated in each of these eight groupings to obtain statistical significance. The effect of increasing the temperature was seen to produce a 5 mV gain in V_{oc} for all groupings, as well as decrease the time necessary to achieve maximum short circuit current. In all cases a fast cool was found to increase I_{sc} with little or no effect on open circuit voltage.

2.2.2 Paste Thickness and Drying Effects

A number of blank wafers were printed with Al paste using screen mesh variations of 165-mesh (the standard), 105-mesh and 80-mesh. The surface condition of the blanks ranged from texturized to chem-polished. The effects of paste thickness and prior wafer condition could be examined for physical differences in the appearance of the back surface field. No observable variance between texturized and polished wafers was ever found, probably due to the 8-10 micron silicon solvation which occurs during the firing. The 80-mesh screen was found to deposit a quantity of aluminum sufficient to dissolve through the silicon, and was thus discontinued from further use.

Using four-point probe readings as an indication of aluminum alloy effects, the quantity of aluminum applied to a wafer surface was found to have an effect only when the paste was dried at the usual 250°C. For this situation the sheet resistance decreased as the aluminum thickness increased. However, drying the paste at 400°C nearly eliminated thickness effects and resulted in uniformly low readings. However, this was not translated into voltage increases on completed cells.

One advantage of the 105-mesh over the 165-mesh is the smoother back surface achieved after paste firing. A 10% reduction in center-line-average surface roughness being typical. This should enhance the effectivenss of a back surface reflector.

2.2.3 Back Surface Preparation

All HESP I paste BSF cells and early HESP II cells were back etched prior to application of the aluminum BSF paste. During this contract a series of experiments

were run to see if this step could be avoided. If so, then a fairly inconvenient process step could be eliminated, enhancing the manufacturability of the HESP cell by reducing cost and breakage. Again 1 ohm-cm wafers were used since they tend to exaggerate BSF problems. A small sample of non-back etched cells were run to see if any BSF enhancement would occur and results were quite encouraging. As a result 32 wafers were broken into two groups; half fabricated with back etching and half without back etching. The two groups were checked electrically after complete fabrication with the following results:

Cell Type	I_{sc} (mA)	V_{oc} (mV)	I_{500} (mA)
back etched	165 ± 1	616± 3	151 ± 7
nonback etched	164 ± 2	616± 2	154 ± 5

Initial examination indicates essentially identical characteristics, consistent with the first experiment and implies that back etching can probably be eliminated. An additional benefit, although not obvious from this limited sample, is the higher average current at load. It was not until an additional group of non-back etched 10 ohm-cm cells were processed that the improved lot average became more evident. It does appear that fewer cells with very low fill factors are occurring with the non-back etched samples. This may reflect the fact that one less step, and consequently less potential damage, is in the new process or it might imply something more basic about the alloying process. The former proposition is felt to be most likely at this time.

Visual examination of the rear surface of the non-back etched cells and back etched cells shows no difference in

smoothness or alloying patterns. Since nearly 8 microns of cell structure are dissolved in the alloying process this is probably not too surprising, and does indicate that welding should not be compromised by elimination of the back etch.

At present numerous cells have been fabricated without back etching prior to the paste BSF application. Cell output power has been consistently good, with a reduced quantity of low output (< 78 mW) cells. However, two problems were noted. The first concerns the formation of heavy phosphorous stains. In some diffusions the wafers became covered with small regions ($\sim$ 1 mm) of highly concentrated phosphorous doped oxide stains. If the aluminum BSF paste is applied over these areas subsequent alloying does not successfully dissolve through these regions, and as a result rough bumps or islands remain. Within these islands phosphorous may compensate the aluminum reducing the P+ effect. In addition, they can prevent the cell from fitting flat on the test fixture leading to difficult electrical measurements. Of even greater concern is that it is not possible to weld to these regions since the structure is granular or porous, not allowing for uniform heating and thereby forming microcracks under the weld.

A solution to this problem is to HF the wafer prior to the aluminum application in order to remove the phosphorous doped oxide glass. Some cells have been processed in this manner with encouraging results; however, it has been the practice up to now to protect the front N+ diffusion from handling damage by leaving on the oxide until the front contacts are applied. Whether the removal of the oxide will introduce more problems cannot be determined from the limited number of cells processed to date with HFing.

An additional area of concern has been that a large portion of the non-back etched HESP cells have recently exhibited a lower V_{oc} (approximately 5-10 mV) than earlier back etched cells. Improved I_{sc} and fill factor have lead to comparable power however. If this additional V_{oc} can be retained with the better process yield, a two percent output improvement would result bringing the 15.3-15.4 percent efficient cells up to 15.5-15.7%. Most recent work with a modified alloy cycle has yielded many high V_{oc} cells and 15.7 percent cells are being pursued.

2.2.4 Back Surface Condition

In order to obtain a back contact suitable for welding and which could aid in back surface reflection, a matrix of aluminum paste materials was tested. The evaluation criteria included smoothness, effectiveness as a back surface field and sensitivity to changes in firing time. In order to increase the severity of this test, one ohm-cm material was utilized. Some of the cells fabricated in this aluminum materials test were included in the third sample cell shipment to WPAFB. Table 1 represents the results of this study. An examination of heating and cooling rates, even as severe as liquid nitrogen quench revealed no advantage in output. Interestingly, silicon hexaboride prevented silicon regrowth, probably by providing nucleation sites so the slight undercooling necessary for material regrowth could not occur. However, there was no change in field effect observed with this very different firing characteristic.

2.2.5 Double Back Surface Field

Review of the HESP program shows that the replacement of an evaporated Al BSF with a non-evaporated Al BSF process

produced a large increase in cell output. And since 1976, evaporated Al has been largely ignored. However, it was decided to reintroduce an evaporated process in order to see if further BSF improvement could be obtained. The approach examined was to evaporate a thin layer of aluminum on the back surface prior to application of the screen printed Al and then alloy the combination. It was felt that the initial evaporated layer might lead to a more uniform alloying with the silicon. In order to magnify the BSF behavior 1 ohm-cm samples were used. Electrical properties for the 9 "double BSF" and 15 control samples are listed below.

Cell Type	I_{sc} (mA)	V_{oc} (mV)	I_{500} (mA)
"double BSF"	168.2 ± 1	619.6 ± 1.9	150.6 ± 8.7
controls	168.1 ± 1.6	617 ± 3.4	150.4 ± 9.3

Electrical characteristics are essentially equivalent indicating that the evaporated layer does not add to the overall BSF effect obtained from the aluminum paste.

2.3 Gettered BSF

It has been proposed that cell efficiency might be compromised by the inclusion of lifetime damaging impurities in low concentrations in the bulk silicon introduced during crystal growth or left over from initial silicon purification. Furthermore, it was possible that this material was being gettered into the BSF region during the alloying cycle, thereby incurring unusually high damage during irradiation which would rapidly degrade the BSF beneficial effects. Therefore if a separate gettering step were implemented prior to BSF formation, and the impurities were removed from the silicon, then improved

TABLE 1

ALUMINUM PASTE SYSTEMS (105 MESH SCREEN)

Paste	Voltage Range	Surface Finish	C.F.F.
Engelhard A3484	595-615	Pitted	.74-.77
Engelhard A3484 + 2% Al_2O_3	595-614	Smooth	.75-.77
Engelhard A3484 + 5% Al_2O_3	604-620	Smooth	.76-.77
Engelhard A3484 + 10% Al_2O_3	604-620	Smooth	.78-.79
Engelhard A3484 + 2% SiO_2	605-622	Smooth	.78-.79
Engelhard A3484 + 5% Si (boron-doped)	595-611	Smooth	.76-.77
Engelhard A3484 + 10% Si (boron-doped)	595-605	Smooth	.76-.77
Engelhard A3484 + 5% $Si\ B_6$	605-622	Smooth	.78-.79
Engelhard A3484 + 2% Al Resinate	604-622	Pitted	.76-.78
Engelhard 3113	605-616	Smooth	.71-.74
Thick Film Systems Al 563	607-622	Smooth	.78-.79
Reynolds 1-131 + Ethyl Cellulose and Terpinal	610-620	Smooth	.78-.79
Alcoa 1401 + Ethyl Cellulose and Terpinal	606-621	Smooth	.78-.79

cell output and radiation resistance might be achieved. Two separate techniques, one using aluminum and the other copper, were examined.

2.3.1 Aluminum Gettering

Based on work performed on Air Force Contract F33615-77-C-2045, aluminum paste appeared to provide the best system for impurity gettering. Although phosphorous gettering and evaporated aluminum gettering had also been examined, the most encouraging results had been achieved with the Al paste. It was decided not to repeat these other techniques on the HESP program, but rather to concentrate on the paste method. Since the original work did not look at gettering in a BSF cell structure, the inclusion of the BSF was felt to be a significant variable that warranted additional study of Al paste gettering.

In order to maximize any gettering benefit 1 ohm-cm material was selected since lower resistivity silicon is expected to contain a greater quantity of lifetime damaging impurities, due to its higher doping levels. For this experiment two groups of eighteen wafers were prepared. The first group was etched slightly so as to remove the initial saw damage (approximately 25 microns per side). This group was then printed with aluminum paste, baked, and alloyed at 850^{o}C for 20 minutes. The time and temperature were felt to allow for sufficient diffusion of any impurities to the aluminum/silicon interface.

Following the gettering the excess aluminum was removed and an additional 50-75 microns per side were removed

from the silicon. This was sufficient to remove the entire alloyed region and any gettered impurities. The wafers were then diffused and processed normally. A second group of wafers was then etched down from the as-sawn condition to a thickness equal that of the gettered cells after all etching. These control wafers were diffused and processed as usual.

Contacts consisted of Al-Cr-Pd-Ag backs and Ta-Pd-Ag fronts, again the same as the conventional HESP cells. TAble 2 lists electrical output characteristics for both groups following Ta_2O_5 AR coating and edge etching. As can be seen the gettered cells do not exhibit any advantages over the controls and are in fact, slightly inferior. Although I_{sc} values are comparable there is a significant V_{oc} difference (8 mV) with a corresponding drop in power at the 500 mV load point. If material lifetime were impacted it would be reasonable to expect a difference in I_{sc}; however this is not the case. The difference in V_{oc} is not readily explained although it may be a matter of handling difficulties. Possibly not all of gettered aluminum was removed during the second etch (local pockets, etc.), and might have introduced some difficulties during the BSF formation which would affect overall device voltage. Again this is a matter of conjecture.

TABLE 2
IMPACT OF ALUMINUM PASTE GETTERING ON CELL ELECTRICAL PERFORMANCE

Cell Type	I_{sc} (mA)	V_{oc} (mV)	I_{500} (mA)
Controls	167.5±1.1	611 ± 4	145.2 ± 8.1
Al Gettered	167 ±1.9	603 ± 6	137.2 ± 7.1

2.3.2 Copper Gettered

Work on another contract, JPL 954694, has shown the usefulness of copper as an intentionally incorporated impurity for neutralizing titanium and other impurities in silicon. To test for the possibility of copper-gettering a sliced wafer, the following experiment was performed: silicon slices of 0.30 mm thickness and 0.05 ohm-cm resistivity were coated on one side with approximately 1000 Å of copper. After copper coverage, the wafers were heated in argon at 900°C for 15 minutes followed by a cleaning in sodium hydroxide to remove copper silicide which had formed on the surface. This cleaning was followed by a 30 minute bake at 850°C to assure adequate time for copper diffusion. This was followed by a subsequent hydroxide cleaning and a control group of the original sample was added to the copper-treated group. All wafers were not diffused and fabricated into solar cells. The copper-treated wafers were further subdivided into a lot which was diffused on the same side as the original deposition and a lot diffused on the reverse side. The final cell testing revealed no difference between any of the groups. All cells having the same curve shape and maximum power. The highest voltage attained was 635 mV.

Although these results cannot be considered as positive, it should be stated that the gettering may not be as effective for non-irradiated silicon. Initially impurities may be relatively inactive electrically. However subsequent particulate irradiation might lead to electrical activation of the impurities, and it would still be worthwhile to include a few gettered HESP samples of each aluminum or copper type in radiation tests regardless of the lack of effect noted above.

2.4 Back Surface Reflector

It was initially proposed that an improvement in the back surface reflector might be achievable with the replacement of aluminum by copper or tantalum. However neither metal proved superior in practice even though theoretical considerations indicated a potential superiority. The copper system failed during the AR coating bake cycle, proving incompatible with any high temperature contact systems. In contrast the use of tantalum as a reflector does not sacrifice high temperature stability, but rather does not lead to any appreicable current gains.

Early in the contract effort a tantalum silver rear contact system was examined. Although tantalum had been non-ohmic for non-BSF backs it was felt that it might become ohmic to the highly doped BSF surface.

For ease of fabrication 10 ohm-cm polished wafers were used with a 2 step diffuse-then-alloy BSF process utilizing an evaporated aluminum source, rather than the present aluminum paste which would entail a longer fabrication cycle not felt necessary at that point. Sixteen wafers were processed as a single group through the diffusion and alloy steps and then randomly divided into 2 equal groups for the contacting. Eight wafers received Ti-Ag backs and were sintered while the remaining eight received Ta-Ag backs. All wafers then received Ta-Ag fronts, Ta_2O_5 AR coatings, a one minute 700^{o}F air bake, and edge etching. AMO I-V measurements proved surprising for although both groups exhibited similar values of I_{sc} and V_{oc} (approximately 145 mA and 580 mV respectively) the Ta back cells all showed evidence of high series resistance with severely reduced fill factors. Series resistance measurements yielded values of up to 1.5 ohms, an order of magnitude greater than normal. At the same time

the control group of Ti back cells fell into two categories; "poor" which were comparable to the Ta back cells and "good" which were tupical of high quality cells, with fill factors of .77-.78, and series resnstances of 0.11 ohms.

The behavior of the Ta back contact cells (and "poor" Ti back contact cells) is not what might be anticipated from a non-ohmic (rectifying) contact. The equivalency of the V_{oc} values is not consistent with the severe fill factor losses, since a loss of V_{oc} would be expected. Rather, an explanation must be offered in terms of high contact resistance, or surface contaminants. The equivalency of Ta-Ag and Ti-Ag back contact voltages and the mixed performance of the Ti-Ag cells, indicates an additional unknown degradation mechanism, rather than a non-ohmic Ta contact has produced the observed results.

However the equivalency of the two cell groups I_{sc} indicates the lack of any significant difference in back surface reflection mechanism. In view of the electrical problems and lack of heightened response Ta was not felt to provide a promising alternative to aluminum.

At this time, then, aluminum has been retained as the back surface reflector. Results to date have consisted of varying process parameters for the aluminum deposition in order to optimize output gains. Since it is necessary to examine the BSR impact on actual cell assemblies the final part of this optimzation effort is being scheduled for the process integration portion of the program.

At the present time an output enhancement of 3.5 mA represents the gain available with an aluminum BSR. This is based on the performance of HESP II type cells with and without a BSR, as shown in Table 3. Eight 10 ohm-cm cells were used in each group.

TABLE 3

EFFECT OF ALUMINUM BACK SURFACE REFLECTOR

	I_{sc} (mA)	V_{oc} (mV)	I_{500} (mA)
No Reflector	170.5	616	160.5
With Reflector	174.0	615	164.0

2.5 Contact Metallizations

2.5.1 Contact Metal Systems

A literature survey was conducted early in the program to investigate the properties of various candidate contact metals. The intent was to ascertain those properties which would tend to maximize high temperature stability, humidity resistance and ohmic electrical behavior. The following properties appear to have importance in choice of materials for use as the base layer (contacting the silicon), the passivation (or intermediate) layer, and the outer (conductive) layer.

1) Base Layer Properties
   a) Generally the higher the melting point of a metal, the higher will be the temperature at which solid state diffusion occurs through the silicon diffused layer, causing shunting effects.
   b) Thickness of the base layer does not appear to be a major factor in preventing outer metallization layers contaminating the silicon diffused layer. Instead, migration along grain boundaries in the base layer is the major mechanism, and with higher melting point materials smaller grain sizes occur which can result in increased contamination problems.

c) Passivation effects may be due to the formation of metal hydrides in the base layer due to galvanic action. (Palladium has greater hydrogen solubility than nearly all metals, and thus acts to improve the integrity of the base layer.)

d) It may be possible with some base layer materials to form nitrides or oxides which could "plug" grain boundaries and prevent transport through the base layer at elevated temperatures.

e) Material transport will be minimized through the base layer if the thermal expansion coefficient of the base layer is a good match for silicon in order to reduce thermal stresses.

f) A compound formation between the base layer and the passivation layer is desirable for good high temperature stability. This also acts to reduce material transport through the base layer.

g) The base layer should form a silicide to provide a good ohmic electrical contact.

h) The dendritic nature of the silicon regrowth layer after back surface field formation by alloying in aluminum may allow faster and deeper penetration by base metals, thus compromizing the BSF structure at higher temperatures.

2. Passivation Layer Properties

a) Passivation layer materials should form silicides to retard transport through the diffused layer if they have penetrated the base layer.

b) A high melting point is desirable to minimize solid state diffusion.

c) Hydrogen absorption is desirable if the base layer is capable of forming hydrides.
d) The passivation layer need be only thick enough to provide humidity protection.
e) Passivation metallization would ideally form conductive layer metal at high temperatures.

3. Conductive Layer Properties

a) The material should be a good electrical conductor with low specific resistivity.
b) It is desirable that the material have hydrogen absorption.
c) Conductive compound formation with the other layer(s) is an advantage.

Table 4 displays the pertinent information needed for the proper selection of a metallization system for contacting silicon solar cells. Table 5 presents a list of the contact metallizations which have been applied to shallow junctions (135 ohms/square), polished, 10 ohm-cm wafers with alloyed aluminum back surface field layers. Investigations of the effects of base layer and passivation layer materials and thickness are now being carried out. Included in the study are base layer nitrides (those that are conductive) where the nature of their structure should provide a barrier to passivation metal migration. The results of these experiments will permit prediction of an optimum metallization system.

Currently a vacuum system is being modified to accommodate the high temperature vacuum bake test setup required for the 260°C and 400°C tests which are a part of this program.

TABLE 4

INFORMATION PERTINENT TO THE SELECTION OF THE OPTIMUM SOLAR CELL METALLIZATION

		Hf	Nb	Ta	Cr	Mo	Ti	Cu	Ag	H_2	Si	Melting Point (°C)	T. C. E. (X 10^{-6}/°C)
	Si											1410	2.5
Conductors	Ag									o	X	961	19.2
	Cu								X	X	X	1083	16.8
Base Layers	Ti							X	X	X	X	1660	8.5
	Mo							*	o	*	X	2617	5.0
	Cr							o	o	X	X	1857	6.0
	Ta							*	o	X	X	2996	6.5
	Nb							o		X	X	2468	7.1
	Hf							X	X	X	X	2227	6.0
Passivation Layers	Rh	X	X	X	X	X	X	X	*	*	X	1960	8.3
	Pd	X	X	o	X	o	X	X	o	X	X	1552	11.6
	Ir	X	X	X	X	X	o	o	*	o	X	2443	6.5
	Pt	X	X	X	X	X	X	X	X	X	X	1769	8.9

Where: X = Compound Formation

o = No Compounds

* = No Solubility

TABLE 5

CONTACT METALLIZATION MATRIX

	Thickness (Å)
Titanium Base Layer	
Materials	
Ti-Ag	1,000 - 40,000
	3,000 - 40,000
Ti-Pd-Ag	1,000 - 400 - 40,000
	3,000 - 400 - 40,000
	1,000 - 1,200 - 40,000
Ti-TiN_x-Pd-Ag	1,000 - 1,000 - 0 - 40,000
	1,000 - 3,000 - 0 - 40,000
	1,000 - 1,000 - 400 - 40,000
	1,000 - 3,000 - 400 - 40,000
Ti-Pt-Ag	1,000 - 400 - 40,000
	1,000 - 1,200 - 40,000
Chromium Base Layer	
Cr-Pd-Ag	1,000 - 400 - 40,000
	3,000 - 400 - 40,000
	1,000 - 1,200 - 40,000
Cr-CrN_x-Pd-Ag	1,000 - 1,000 - 0 - 40,000
	1,000 - 3,000 - 0 - 40,000
	1,000 - 1,000 - 400 - 40,000
	1,000 - 3,000 - 400 - 40,000
Cr-Pt-Ag	1,000 - 400 - 40,000
	1,000 - 1,200 - 40,000
Tantalum Base Layer	
Materials	
Ta-Pd-Ag	1,000 - 400 - 40,000
	2,000 - 400 - 40,000
	1,000 - 1,600 - 40,000
Ta-TaN_x-Pd-Ag	1,000 - 500 - 0 - 40,000
	2,000 - 500 - 0 - 40,000
	1,000 - 1,000 - 400 - 40,000
	2,000 - 1,000 - 400 - 40,000

TABLE 5 (CONT'D.)

Tantalum Base Layer (cont.)	Thickness (Å)
Materials	
Ta-Pt-Ag	1,000 - 400 - 40,000
	1,000 - 1,200 - 40,000
Molybdenum Base Layer	
Mo-Ag	1,000 - 40,000
	2,000 - 40,000
Mo-Pd-Ag	1,000 - 400 - 40,000
	1,000 - 1,600 - 40,000
	2,000 - 400 - 40,000
Mo-MoN_x-Pd-Ag	1,000 - 500 - 0 - 40,000
	2,000 - 500 - 0 - 40,000
	1,000 - 1,000 - 400 - 40,000
	2,000 - 1,000 - 400 - 40,000
Mo-Pt-Ag	1,000 - 400 - 40,000
	1,000 - 1,200 - 40,000
Palladium Base Layer	
Pd-Ag	1,000 - 40,000

All of the necessary mechanical and electrical feed-throughs have been installed and the heater assembly fabricated. Quartzline lamps to be used for heating the cell assemblies in the vacuum chamber are ready for installation. An appropriate temperature monitoring system is being designed to accurately measure the cell assembly temperature during the test.

2.5.2 Humidity Testing

An extensive matrix of contact metallizations where an aluminum back surface reflector was present has been subjected to an accelerated humidity test. An aluminum (only) metallization survived this accelerated testing, but all other combinations displayed signs of deterioration with blistering or contact separations. The metal systems tested were:

Al-Pd-Ag	Al-Ti-Pd-Ag
Al-Ag	Al-Cr-Pd-Ag
Al	Al-Pd-Cr-Pd-Ag

The last metal combination listed above appeared to be more resistant to humidity damage than the others.

Additional tests were performed on metallization systems which were found to be compatible with an aluminum back surface reflector after humidity. These included:

Al-Cr-Pd-Ag
Al-Pd-Cr-Pd-Ag
Al-Mo-Pd-Ag

The chromium apparently functions where titanium fails due to a polarization layer established during exposure to humidity. This layer acts to limit the galvanic currents. Of the three systems above, the molybdenum metallization performed the best after exposure to humidity.

2.5.3 Evaporation Masks

Appropriate bimetallic masks were designed and ordered early in this program. Due to long lead times and design changes recommended by the mask fabricator actual cell production using these masks was delayed and the grid configuration was not evaluated until the eighth month of effort. Although the gridline and ohmic bar configurations are identical for both the 2 x 2 cm and 2 x 4 cm cells processed had slightly lower power points, mainly due to a reduced fill factor. This may have been the result of slightly different handling techniques for the larger cells. No real problem is anticipated, however, in obtaining comparable outputs for the two sizes.

The bimetallic masks were designed to the grid configuration specified in MIL-C-83443A, and provide for two ohmic weld pads that are a minimum of 4.000 x 8.000 mm in size. Our interconnect weld tab area is much smaller than the pad size designed into the mask, and thus some active area is lost to this specification. A sketch of the 2 x 2 cm cell contact configuration is shown in Figure 3.

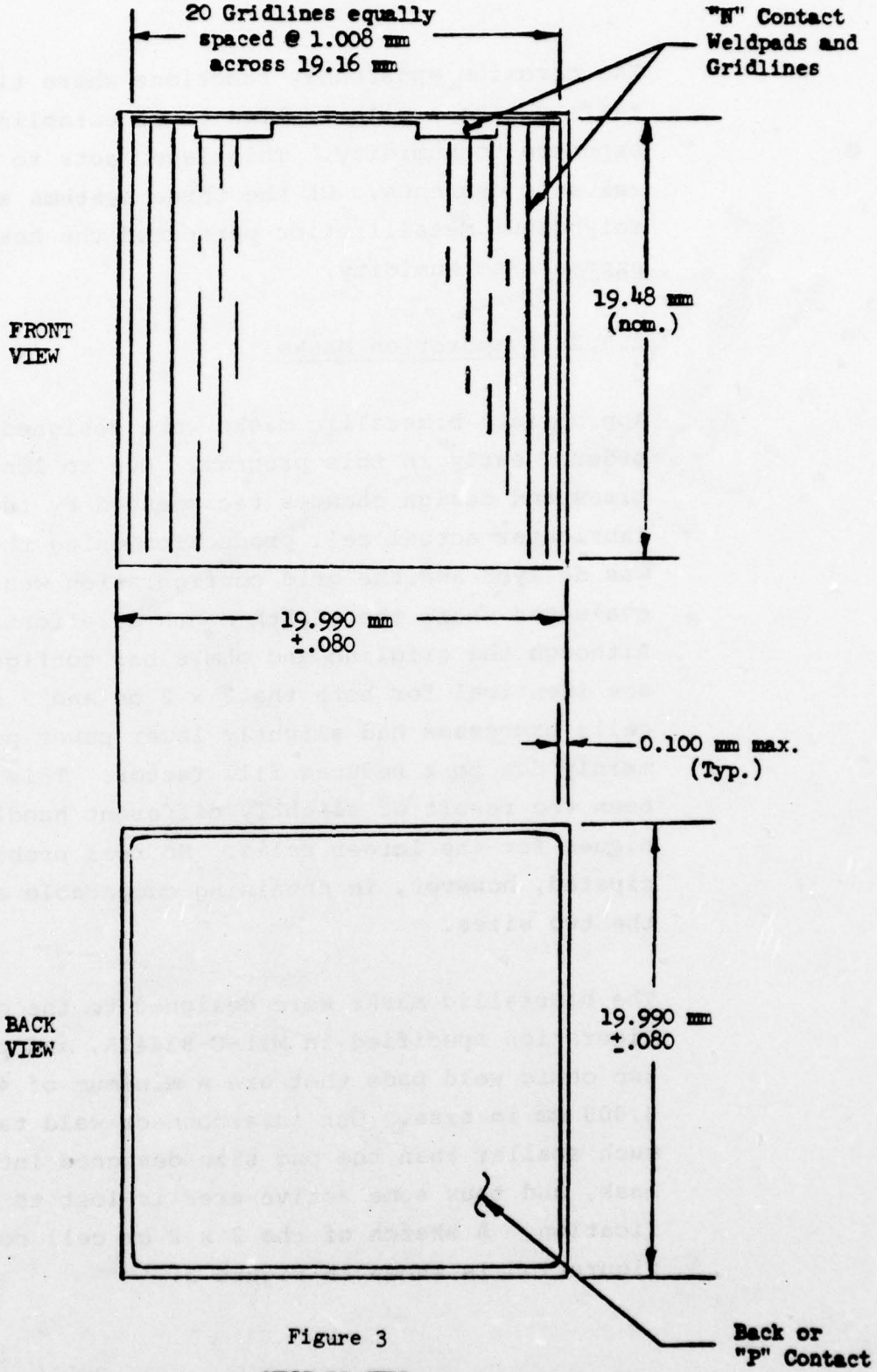

Figure 3

HESP-II CELL

2.6 AR Post Treatment

s stated in the original proposal it is possible that the Ta_2O_5 AR coating efficiency could be improved through the use of higher temperature baking processes. Such baking has been shown to provide an increase in cell short circuit current through increases in transmission at short wavelengths and increases in the refractive index (improved I_{sc} after filtering). However the high back temperatures required to fully optimize the coating behavior degraded the cell output, even though the more reactive titanium layer was replaced with tantalum. Work on another contract, JPL 954694 has shown that palladium, which is needed for humidity resistance, is highly damaging in silicon, so possibly this material limits the high temperature resistance of the HESP cell.

It was felt that if a deeper diffusion could be used, the contact metals might not migrate into the junction region under a high thermal exposure, and an optimized AR coating would be achieved.

However, considerable work on the HESP program and other projects has demonstrated the importance of shallowing the N+ diffusion in order to maximize the solar cell short wavelength response, and provide maximum power after particulate irradiation. With the diffusion process used at Spectrolab a junction depth of approximately 0.1 microns provides an optimized output, with further reduction yielding from marginally higher to lower cell output.

Literature surveys indicate that it may be possible to modify the diffusion so as to obtain an optimized short

wavelength response and relatively deep junction simultaneously.[4] Furthermore, additional gains may possibly occur in cell open circuit voltage, and fill factor.[5]

The mechanism for achieving this is to lower the maximum impurity concentration of the emitter diffusion. Benefits here would be manyfold. Lifetime in the diffused N+ region, γ_p, has been demonstrated to follow the empirical relation:

$$\gamma_p = \frac{\gamma_O}{1 + \frac{N_D}{N_O}}$$

where γ_O and N_O are constants normally determined from experiment. Values from reference (1) are 3.5×10^{-7} sec and 7.1×10^{15} cm^3 respectively. For the silicon cell processes presently employed the diffusion phosphorous concentration N_O, varies from 10^{20} atoms/cm^3 at the surface to the bulk silicon value (10^{14} to 10^{16} atoms/cm^3. At the highest level the calculated lifetime is 6×10^{-12} sec, increasing to 2.5×10^{-11} sec at 10^{20} and 2.4×10^{-10} sec at 10^{19} atoms/cm^3. Due to the extremely short lifetime near the surface, it is necessary to have a shallow junction in order to collect the carriers generated just below the surface. If the surface concentration is reduced, then the increased lifetime will allow carrier collection with a deeper junction. In addition high doping levels are felt to decrease the cell voltage, since dopant energy level broadening will occur at high concentrations effectively reducing the diode band gap. Hence at high dopant levels there is a saturation which leaves an effective level of approximately 5×10^{18} atoms/cm^3. Higher levels provide conductivity gain, but lead to lifetime and band gap loss.

With this in mind a low phosphorous concentration liquid spin on surce was selected that would provide a surface concentration of 3×10^{19} atoms/cm^3, for a one order of magnitude reduction. Although a lower concentration would be better on theoretical grounds, it was felt that this intermediary level would be easier to integrate with the standard Spectrolab processes, minimizing possible problems anticipated with the higher sheet resistances (due to the lower maximum concentration the sheet resistance for a given junction depth would increase).

Manufacturer's data indicated that a .3 micron junction depth could be obtained at 850^{o}C with a sheet rho of 150 ohms/square. So the same diffusion parameters were followed, and processed cells examined. It was noted immediately that cell current and voltage were lower than usual. (With the current reduction estimated to be 9 percent and the voltage loss 10%.) Spectral response showed an appreciable loss in long wavelength response indicative of bulk lifetime degradation.

The experiment was repeated with slightly better, albeit still inferior results. This was followed by a month of experiments and periodic conversations with the dopant manufacturer to try to remedy the lifetime problem. Changes in ambient atmosphere during the diffusion were examined along with changes in the diffusion temperature. For a period of time it appeared that increasing the diffusion temperature might improve lifetime. It had been noted earlier, that when the diffused layer for 850^{o}C diffusions was examined it was difficult to get consistent V/I readings. Subsequent hotpoint probing showed the diffused N+ surface to often read as <u>strong P type</u> under ambient illumination even though the undiffused bulk would read slight P type (10 ohm-cm), although the fabricated cells would exhibit the type of I-V curve expected of an N+/P diode structure.

At 900°C firing, the V/I reading became more consistent, and the hotpoint probe readings indicated N type. The first group of cells at this temperature showed only marginal losses in I_{sc} and V_{oc} (less than one percent). However subsequent 900°C experiments were not as good with losses closer to 3 percent or more. Additional firings up to 950°C have, if anything, shown greater lifetime loss than the 900°C fired cells, although the V/I and hotpoint probe readings have been normal. So at that point the low concentration diffusion cells were not electrically equivalent to conventionally diffused cells, with one exception. The short wavelength response of low concentration devices was higher than equivalent depth standard diffusion devices. Further experiments indicated that a low concentration device with X_j = 0.2 microns will have a short wavelength response equivalent to a conventionally diffused wafer with X_j = 0.1 microns.

In view of the promising short wavelength spectral response further studies were continued resulting in a process for junction formation that did not incur long wavelength response losses. Whether such losses were due to actual bulk lifetime reduction or to unusual junction characteristics was not completely clear; however it was not possible to obtain long wavelength response comparable to standard PH_3 diffused cells.

The process changes instituted consisted of the following:

a) Minimize the length of time between coating application and bake and the diffusion;
b) Diffuse at temperatures of 900°C or greater;
c) Diffuse in a nitrogen ambient; and
d) Slow cool the wafers to 650°C following the diffusion.

Since the high temperature-slow cool process now tended to produce deep diffusion (∿1 micron) a lower concentration source of $8 \times 10^{18}/cm^3$ was tried in order to improve the short wavelength response. Three separate tests were run between 900°C and 930°C diffusion temperatures, but it was not possible to get any meaningful cells with the lower concentration source although no problems occurred with 3×10^{19} source samples included for comparison. As an example, open circuit voltages for 1 ohm-cm material with an 8×10^{18} diffusion generally fell in the range of 100 to 400 mV, whereas 3×10^{19} diffusions were measured at 585 mV.

Rather than attempt to redefine a process for the 8×10^{18} source material, it was felt more worthwhile to concentrate on the 3×10^{19} material and improve cell characteristics, in particular the slightly depressed V_{oc} (∿10 mV) values that had been noted when compared to control PH_3 cells. Examinations of the I-V characteristic did not show any indication of low shunt resistance which might otherwise reduce the V_{oc}. It was felt that the problem might be one of a front contact-diffusion barrier.

In order to see if the contacts might be involved in the problem two spin-on groups were fabricated into cells, one with Ta-Ag contacts (used on all previous groups) and the other with Ti-Ag contacts. Suppressed voltages were noted in both cases. Normally the Ta-Ag contact requires heating to become ohmic. This occurs during the 700°F AR coating air bake. A number of the Ta-Ag cells were reheated at a higher than normal temperature (900°F) for one minute. Both I_{sc} and V_{oc} were found to increase slightly. It was decided to continue baking at even higher temperatures,

and cell output increases continued as the bake temperature was increased up to 1060°F (570°C) Baking at this temperature continued providing a slight improvement for up to seven minutes' exposure. The total maximum gain at this temperature was 6 mA (4.7%) and 13 mV (588-601 mV). Results of this bake treatment are summarized in Table 6.

Similar tests were performed with the Ti-Ag group with essentially equal results. Since Ti-Ag normally does not require a bake treatment for the front contact to become ohmic, this was surprising. Ti-Ag contacts are known to degrade cell curve shape faster than Ta-Ag when heated due to the formation of titanium silicides and impurities. Hence prolonged baking (7-10 minutes) did begin to degrade the cell although this was considerably more resistant than a conventional PH_3 diffused cell. The fact that the deep diffusion ($\sim$1 micron) spin-on source cells did degrade during the high temperature bake does point out the great distance impurities/silicides traverse at these temperatures.

This sequence of tests points out a number of interesting results. First is the ability to achieve V_{oc} equal to or higher than PH_3 diffused samples. Second the total AR coating enhancement was 43% greater than the uncoated cell -- 39 to 41% is more typical. And thus, the spin-on cells were able to withstand nearly 600°C exposure for over 5 minutes with little or no loss in fill factor. The voltages indicate that any contact barrier can be eliminated by a high temperature bake. Such a treatment may be necessary due to the lower dopant surface concentration. The AR enhancement which was consistent with the gains originally

proposed, indicates that a higher post coating bake temperature does provide a better Ta_2O_5 coating. The stability of the cells at high temperatures would indicate superior laser resistance and possibly an ability to undergo in situ very high temperature radiation damage annealing.

Prior to the high temperature bake testing, an unusual behavior pattern was noted for the sample cells. As each cell remained illuminated by the xenon source during electrical output testing the V_{oc} and I_{sc} would slowly decrease. During the period of the actual measurements this was quite slight. However, leaving a few cells illuminated deliberately for extended intervals, the magnitude of the loss became quite appreciable with drops of 2 mA and 4 mV occurring within five minutes. Concern with possible photon degradation lead to subjecting a sample to 20 hours continuous AMO illumination.

The cell was initially measured at 125 mA I_{sc} and 588 mV V_{oc}. Immediately following the 20 hours of illumination the I_{sc} had dropped to 120 mA and the V_{oc} to 584 mV. The cell was removed from the fixture and then retested after one hour of room ambient (fluorescent) illumination. The I_{sc} was now up to 126 mA and the V_{oc} at 588 mV, for complete recovery. Following this the cell was subjected to the high temperature bake cycle after which the I_{sc} was measured at 130 mA and the V_{oc} at 599 mV. The impact of subsequent illumination was not nearly as pronounced as had occurred earlier. Apparently the prebake losses are related to the contact barrier problem and the reversible nature of the problem may indicate some sort of charge accumulation at the contact silicon interface. Efforts to eliminate the instability problem by high temperature baking met with reasonable success; however, the

Table 6

IMPACT OF ELEVATED AND EXTENDED BAKE TEMPERATURE
ON I_{sc} AND V_{oc} OF 3×10^{19} DIFFUSION CONCENTRATION CELL

Process Condition	Average I_{sc} (mA)	Average V_{oc} (mV)
A. Finished cell with normal Ta_2O_5 bake ($700^{\circ}F$)	125.9	588
B. 1 minute additional bake at $1060^{\circ}F$	128.6	594
C. 3 minute total bake at $1060^{\circ}F$	130.7	599
D. 7 minutes total bake at $1060^{\circ}F$	132.2	601

fact remained that even though higher AR coating efficiency was achieved by means of the extended high temperature bake, the low concentration spin-on process was not compatible with high short wavelength response. The need for a high temperature diffusion and slow cool cycle meant that the junction depths obtained were always deeper than optimum.

2.7 Interconnects and Welding

A review of the technical requirements/tasks of this program with regard to tests on cell assemblies and modules required some deviation on the temperature ranges. Rather than the requirements as noted in MIL-C-83443-A, the temperature cycling requirements were aligned more to that of normal tests done at Spectrolab on its aerospace qualified modules and assemblies, i.e., $+150^{o}C$ to $-180^{o}C$ with a maximum rate of $25^{o}C$ per minute.

A preliminary investigation using a 0.025 mm thick silver mesh with weld schedules used in HESP-I was tried on HESP-II cells. Generally the weld schedules used earlier gave good pull strengths, (700 grams) for both front "N" contacts and back "P" contacts with less than 1% loss of output power at approximately maximum power.

A molybdenum metal interconnect previously designed for HESP-I cells, was processed through a silver plating procedure to yield one sheet each of 7 microns and 15 micron thick plated silver surfaces.

Initially a modified silver mesh weld schedule was tried on the molybdenum/silver plated interconnect. However even after many deviations from the mesh weld schedule, no acceptable pull strengths could be obtained.

After some investigation into early HESP-I weld data, a weld schedule was tried where tip pressure was decreased to 1.3 kg (0.6 pounds) compared to normal silver mesh pressure of 3.32 kg (1.5 pounds). The tip spacing was increased to 0.533 mm from 0.25 mm. Initial "N" contact welds made at 0.78 to 0.82 volts and 80 milliseconds pulse width, showed good pull strengths (750 grams). Since the initial BSF surface was very rough and inconsistent, this was transferred to weld pull strengths, which, for a given weld schedule, gave erratic pull results. However a new technique of BSF firing gave cells a much smoother and uniform BSF surface finish whereby a single weld schedule of 0.89 volts and 80 milliseconds pulse duration gave uniform pull strengths.

Having established a uniform pull strength in excess of 500 grams vaerage, the maximum power degradation of the cells was looked at. Again, as experienced in HESP-I, the maximum power is affected quite drastically by the "N" contact welds but negligibly by "P" contact welds. Slight weld schedule changes from those initially looked at gave good pull strengths, about 500 grams average, and a maximum power degradation of ± 1%. These pull strengths and power deviations were based on two welds on "N" contacts and three welds on "P" contacts.

Since the majority of cells to be shipped to WPAFB on this contract are cell assemblies, i.e., with coverglass completely covering "N" welded tabs, a few cells were welded with the molybdenum interconnect and given to Spectrolab's cell filtering group for coverslide bonding using DC 93-500 adhesive. Due to the "tilting" of the coverslide over the interconnect ($\sim$0.025 mm) there was a possibility of air

bubbles being trapped along the interconnect perimeter. However upon curing of the adhesive, no apparent air bubble entrapment was visible under the coverslide.

Due to the extreme test conditions of the cell assembly, i.e., 400°C for 100 seconds at a vacuum of 10^{-5} torr or better, Dow Corning[6] was contacted for a recommendation of an adhesive that would endure these test conditions. There does not now exist any type of adhesive suitable for coverslide bonding that is guaranteed for the test conditions as set forth in our SOW. However, it was felt that with the special care in our adhesive curing procedure, the conditions mentioned previously could possibly be met. A very limited number of samples were prepared for this test and is awaiting the test setup as described in an earlier section.

The welded interconnect design is different from all of Spectrolab's production type soldered interconnects. A new stress relief bend fixture was designed and fabricated to accommodate this new design. A few cells with the stress relief bend in the interconnect were given to the cell filtering group to see if the stress relief bend would cause other unforeseen problems during the filtering process. However, as before, no difficulty was encountered.

Another area that was investigated with additional work pending was that of interconnecting the back "P" contact interconnect in a parallel mode. Since each cell assembly will be individually processed with "N" welded interconnects, a scheme needed to be devised to connect cells in a parallel string without causing electrical degradation while maintaining good mechanical pull strengths. Initial welds

were made along the perimeter of the oval shaped interconnect where the area under the weld tips was similar to the other "P" contact welds and therefore the same weld schedule could be utilized. However since the oval shape was meant to provide stress relief, pull tests at 45^{o} angle and tangent to the weld could not be done. Pull tests on this type of weld sheared off pieces of silicon as the welded area was put into a rotational mode on a plane parallel to the cell surface. Where normal pull strengths using this weld schedule resulted in pull strengths in excess of 500 grams, the "oval" interconnect welds failed at 200 to 300 grams in every instance.

However after some experimentation, it was found that by changing the weld schedule, a weld could be made at the very end point of the oval and these welds appear to yield pull strengths similar to the normal "P" welds. The initial welds evaluated did not appear to degrade the maximum power output of the cells, however additional evaluation will need to be done to insure that electrical degradation does not occur with the revised weld schedule.

2.7.1 Filter Glass

After much discussion with Spectrolab's cell filtering group, it was decided to use a ceria doped coverglass for HESP-II assemblies. Rather than using a quartz filter with an expensive cut-on filter evaporated on one side, the ceria doped glass has a natural cut-on at approximately 310 μm. Alto the transmission of the ceria doped glass after irradiation with 10^{15} 1 MeV equivalent electrons reportedly degrades the least among the conventional materials used in coverslide applications. Thickness of the filters will nominally be 0.152 mm (6 mils).

The first coverslides were attached to the cells using the standard Spectrolab curing time and temperature. A second set of cells which had "N" interconnect welds used a long, low temperature cure. These cells are now awaiting the high temperature-high vacuum test.

2.8 Radiation Screening

An electron irradiation of 1×10^{15} equivalent 1 MeV electrons was used to compare CZ and FZ material of 10 ohm-cm bulk resistivity prepared with texturizing, aluminum paste back surface fields and aluminum back surface reflectors. There was little difference in BOL outputs between CZ and FZ material. Immediately following irradiation the FZ material was nearly 4% higher in output. There was some room temperature annealing which occurred for the CZ material resulting in an output increase of approximately 2%. The FZ material did show some photon induced degradation both under loaded and open circuit conditions amounting to approximately ½%. The CZ material did not show a photon sensitivity. An anneal at $60^{\circ}C$ for 48 hours removed the photon induced damage from the FZ material and had no effect on the CZ wafers. The FZ cells were thus approximately 2% higher in output than CZ cells after an anneal and twenty-four hours of illumination.

During the same irradiation, a few samples of 1-1-1 orientation silicon were tested for degradation. There was no statistically significant difference in output loss between the 1-0-0 and 1-1-1 cells.

A second FZ ingot was ordered from Wacker in order to set up a second screening test to verify the initial results. This ingot was sliced into wafers and cell fabrication was begun during April.

The fabrication was the same as used on crucible grown silicon HESP samples, with the exception of the BSF aluminum paste application. Since the FZ material was received as a 3 inch ingot and since the paste BSF pattern is a 1.88 inch diameter circle maximum wafer utilization required the application of two overlapping paste patterns resulting in a ∞ pattern which allowed the cutting of three 2 x 2 cm wafers. The paste was baked to remove solvents after each circular application.

The first group of twelve (12), 2 x 2 cm FZ cells was tested after fabrication and found to be quite low in output, with an unusually large spread in open circuit voltage. Values varied from 547 to 597 mV, well below the values obtained from comparably processed CG wafers. No correlation could be observed between the amount of aluminum originally applied on the backs, i.e., cells showed little difference if located on a region of one pass of Al or two (the overlap region).

In order to ascertain if some processing error had occurred a second batch of 31 FZ cells were run. In this case much better results were obtained, although still inferior to the CG material in I_{sc} and V_{oc}. Maximum power was approximately five milliwatts below comparable crucible grown lots.

In addition, a large spread in output was again observed, with only 4 cells over 80 mW (one at 83 mW). This lead to the question of material quality and a group of polished FZ wafers were fabricated without use of a BSF in order that some comparison to conventional CG cells could be made. After Ta_2O_5 coating and edge etching these sixteen samples showed an I_{sc} of 148 ± 2 mA and a voltage of 555 ± 4 mV. The former value is felt to fall within the range

of CG grown samples, but the voltage is approximately 10 mV low. A four point probe check shows the FZ material to definitely read 10 ohm-cm bulk resistivity, so that it must be concluded that somehow the method of ingot formation has compromised the material properties. The immediate result of this is that a greater quantity of FZ wafers will need to be processed in order to obtain a satisfactory number of high efficiency cells. Second, it is questionable to consider these cells as typical of FZ cells. Then again, the variation in results obtained with float zone samples to date may be due in large part to subtle variations in the starting material.

SECTION III

CONTRACT INTERIM STATUS

The progress to date has been centered around attacking a number of individual task areas, as described above. Some of those areas have lead to definite cell improvements such as the BSF work, while others have not produced significant changes, such as prediffusion surface treatments. The HESP-II cell uses the final HESP-I cell work as a baseline. An analysis of that program's status at completion lead to the determination of potential areas for improvement and the magnitude of improvement feasible. The results of that analysis are shown in Table 7.

The interim report marks the end of the initial optimization phase on this contract. During the next phase these individual developments will be fully integrated into an optimized structure with complete characterization of the resultant device. The representative sample cells fabricated during this initial contract effort, generally represented the state of the art during each two-month effort. This was not always the case because in some instances samples represented very particular optimizations and do not include all high efficiency aspects. A complete list of all samples with selected electrical characteristics is shown as Table 8. Some typical I-V characteristics are shown in Figures 4 and 5. It is evident that cell output presently falls midway between the HESP-I cell and the HESP-II cell goal. And although overall cell performance seems little changed over the program duration it is interesting to note that the output currents have increased while the output voltage has decreased in an equivalent amount during this same period. This reflects changes in cell processing steps and does not imply that high current and high voltage are mutually exclusive.

Analysis of the representative cell performance can indicate where the HESP-II cell final output will most likely be following process integration and optimization. Sinece not all samples were necessarily SOTA we have selected the most recent 10 cell samples for our analysis.

The most recent ten-cell sample varied in thickness from 5.2 to 6.6 mils as measured by a micrometer. Cell weight, a more accuract indicator of cell thickness due to the uneven cell surface, varied from 115 to 146 mg. Allowing 12 mg for contacts this corresponds to 4.1 to 5.4 mils of silicon respectively. In view of the radiation behavior obtained with the BSF structures, the present thickness is considered a reasonable compromise between BOL and EOL power goals.

All cells are textured with a Ta_2O_5 AR coating, Ta-Pd-Ag front contacts, an aluminum BSR, and Cr-Pd-Ag rear contact. Particular variables represented in the latest group of 10 cells delivered to WPAFB, include full back contact, a BSF without back etch, and ten percent thicker AG metallization. Under AMO conditions, 25°C, the group electrical performance is:

	I_{sc} (mA)	V_{oc} (mV)	P_{max} (mW)	F.F.	efficiency %
average	175.4	604	82.6	.78	15.3
Standard deviation	1.3	4	0.7	.01	.1

It is interesting to examine what the output of a cell would be if it consisted of the high end of the above electrical parameters. This would give I_{sc} = 176.7 mA, V_{oc} = 608 mV, and F.F. = .79 for 84.9 mW or 15.7 percent efficiency. With a typical enhancement of 2 percent from filtering this would yield 16.0%.

Table 7

Phase II HESP 2 x 2 Assembly Power Projection									
Development Area	Pessimistic			Realistic			Optimistic		
	I_{sc} (mA)	V_{oc} (mV)	FF	I_{sc}	V_{oc}	FF	I_{sc}	V_{oc}	FF
Pre-diffusion treatment	0	0	0	0	0	.005	1.0	5	.01
Gettered BSF	0	10	.01	2	15	.015	4	20	.02
Improved Contact Pattern	2.5	0	0	4	0	0	5	0	0
Back Reflector	2.5	0	0	3.5	0	0	4.5	0	0
AR Improvements	0	0	0	1.5	0	0	2.5	0	0
Totals	5.0	10	.01	11.0	15	.02	17.0	25	.03
+									
Phase I HESP	168	600	.78	168	600	.78	168	600	.78
Phase II HESP	173	610	.79	179	615	.80	185	625	.81
Power (mW)		83.4			88.1			93.7	

Table 8

REPRESENTATIVE SAMPLE POWER PERFORMANCE

Cell Number	I_{sc} (mA)	V_{oc} (mV)	P_{max} (mW)	η (%)	F.F.	Comments
1	173	616	83.6	15.4	.78	
2	174	612	82.6	15.3	.78	
3	175	613	84.1	15.5	.78	
4	174	606	82.6	15.3	.78	
5	174	613	83.1	15.4	.78	
6	174	613	82.6	15.3	.77	
7	174	615	81.6	15.1	.76	
8	173	615	83.6	15.4	.79	
9	172	609	82.6	15.3	.79	
10	171	616	84.1	15.5	.80	
11	160	612	76.0	14.0	.78	
12	160	615	76.0	14.0	.77	
13	159	612	75.0	13.8	.77	
14	159	611	75.0	13.8	.77	
15	158	611	75.0	13.8	.78	
16	172	612	81.5	15.1	.78	
17	174	612	82.0	15.2	.77	
18	171	613	82.0	15.1	.78	
19	174	611	81.5	15.1	.77	
20	172	612	81.5	15.1	.77	
21	156	606	75.0	13.8	.79	Junction Etch-Back; HESP I Bar Ohmic Tooling
22	158	607	75.0	13.8	.78	Junction Etch-Back; HESP I Bar Ohmic Tooling
23	156	606	74.0	13.7	.78	Junction Etch-Back; HESP I Bar Ohmic Tooling
24	159	605	75.5	14.0	.78	Junction Etch-Back; HESP I Bar Ohmic Tooling
25	159	607	75.0	13.8	.78	Junction Etch-Back; HESP I Bar Ohmic Tooling
26	162	612	78.5	14.5	.79	No BSR; HESP I Bar Ohmic Tooling
27	163	611	79.0	14.6	.79	No BSR; HESP I Bar Ohmic Tooling
28	165	613	80.0	14.8	.79	No BSR; HESP I Bar Ohmic Tooling
29	163	610	78.5	14.5	.79	No BSR; HESP I Bar Ohmic Tooling
30	162	611	78.5	14.5	.79	No BSR; HESP I Bar Ohmic Tooling
31	172	613	82.4	15.2	.78	
32	172	615	82.0	15.2	.78	
33	172	613	81.6	15.0	.77	
34	173	610	82.0	15.1	.77	NH_4OH Precontact clean
35	173	611	80.6	14.8	.76	NH_4OH Precontact clean
36	173	609	81.2	15.0	.77	
37	174.5	609	83.2	15.4	.78	
38	174	612	82.8	15.3	.78	
39	172	608	82.0	15.1	.78	
40	175	609	82.5	15.2	.77	
41	172	614	83.3	15.4	.79	
42	175	603	82.4	15.2	.78	
43	175.5	606	83.1	15.4	.78	
44	176	602	83.0	15.3	.78	
45	177	604	83.5	15.4	.78	
46	175	602	82.1	15.2	.78	
47	176	603	81.9	15.1	.77	
48	176	602	82.9	15.3	.78	
49	176	602	82.1	15.2	.77	
50	175.5	600	81.5	15.1	.77	

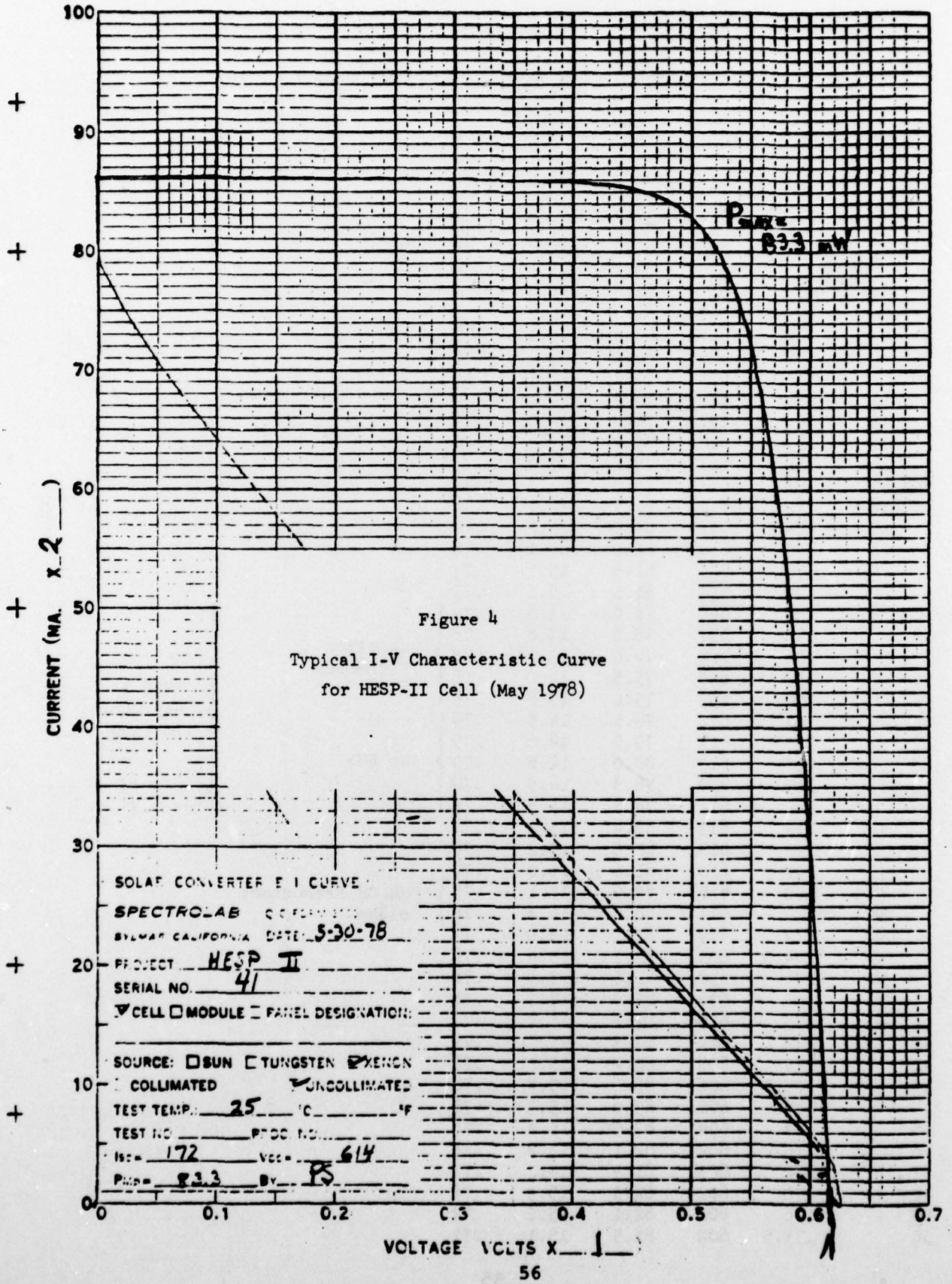

Figure 4

Typical I-V Characteristic Curve
for HESP-II Cell (May 1978)

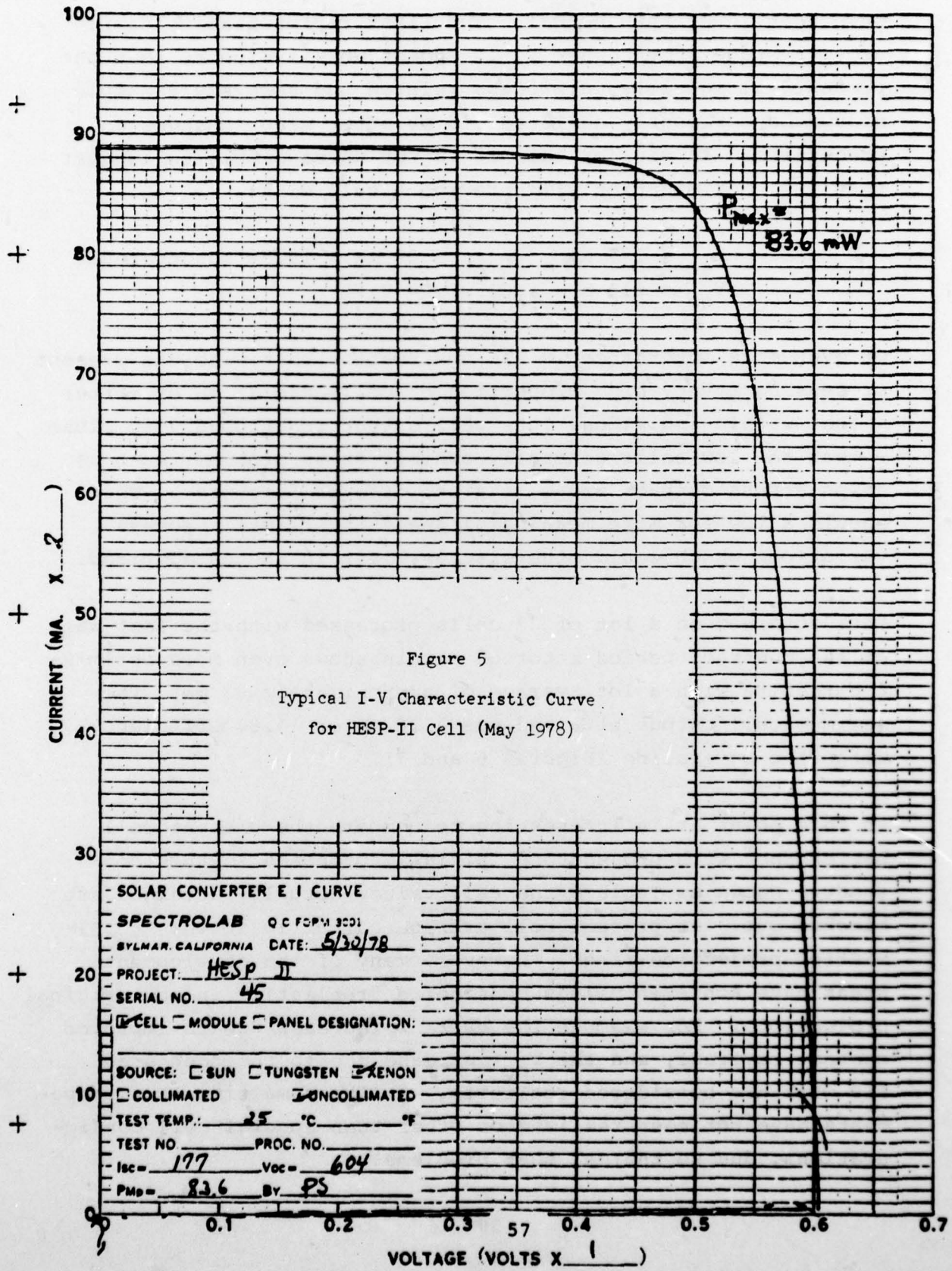

Figure 5

Typical I-V Characteristic Curve for HESP-II Cell (May 1978)

As mentioned earlier, V_{oc} values for the most recent cells have been lower than normal. The first representative sample group average 9 mV higher V_{oc}. Recent work indicates that the present voltage loss is process related and some small sample groups have recently achieved 615 mV after minor changes in procedures. In view of this it is not unreasonable to suggest that full optimization will provide a cell with:

I_{sc} = 177 mA P_{max} = 86 mW = 15.9% (uncovered)
V_{oc} = 615 mV C.F.F. = 0.79

Of even more importance is the observation that with the present processing a very high proportion of cells are 81 mW or better - that within individual lots cell output is grouped very close - that the low cells generally exhibit gross problems such as chips across contact areas, stains, or even fractures. This should allow for more meaningful analysis of small process variations which would otherwise get lost in the data apread.

Data obtained on a lot of 22 cells processed with the last week of the contract period reported herein shows even more optimistic results with a lot average of approximately 83 mW. The maximum cell output attained was 85.6 mW or 15.8% efficiency, without a coverslide (Figures 6 and 7).

At this point it is interesting to compare the present cell performance with projections initially proposed in this contract. Shown as Table 9 the cell values actually attained are blocked out. At present cell average output is in the "pessimistic" projection range. However, many of the development areas have achieved values considered "realistic" in our original projections. For example the current increase due to improved contact coverage, and the V_{oc} increase due to the "gettered" BSF work are considered realistic. At the same time AR improvements have not been realized on other than special cell configurations, due to thermal soak problems.

A cell meeting the goal of 16% or better is considered technically possible. It will now require a gentle optimization of present technology to provide a cell with a configuration of high characteristics. At the same time, some new approaches are bound to be suggested during the process integration stage which might result in an additional 2-3 mW output.

In the realm of dramatic increases we must consider work on another WPAFB contract, F33615-77-C-2045, which by providing ultra-pure material could lead to a dramatic increase in cell output both BOL and EOL. As mentioned earlier FZ silicon has exhibited a rather erratic history, with both promising results and disappointing results. It is reasonable to consider that difficulties with FZ silicon lie in contaminants that reside in the bulk and that removal of these contaminants to some low level will provide a significantly better cell, BOL and EOL. If such material can be realized, optimistic projectures for the gettered BSF and back reflector gain, would be possible in FF, I_{sc} and V_{oc}. This in turn would provide an additional 5 mW or so of output power.

The present HESP cell, 0.10-0.15 mm thick 10 ohm-cm silicon, with a textured front, Ta-Pd-Ag contacts, aluminum BSF, aluminum BSR, and Cr-Pd-Ag rear contact, is now being fabricated with 83 mW power output for a 2 x 2 cm configuration. For a larger size (2 x 4 cm) 82.5 mW power equivalents have been achieved as shown in Figure 8. Rational process integration and optimization can produce a 2 x 2 cm cell with an 86-87 mW power output. Within the very near future better silicon material will become available, which can very possibly provide us with an uncovered 91 mW (16.7%) device. The power increase realized by HESP-I cells over conventional ones may again be attained by the HESP-II pure silicon cell.

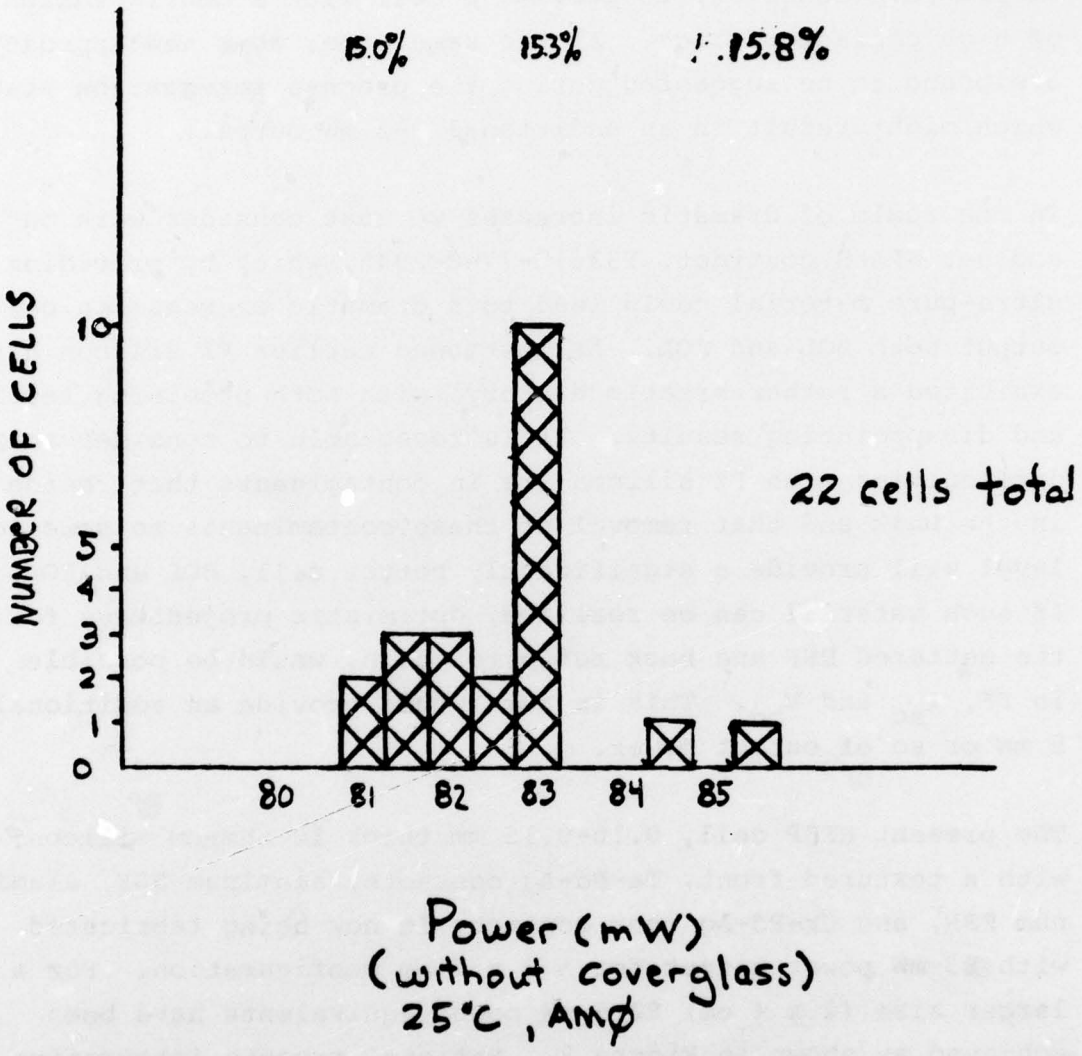

Lot power distribution 6/ 178

Figure 6

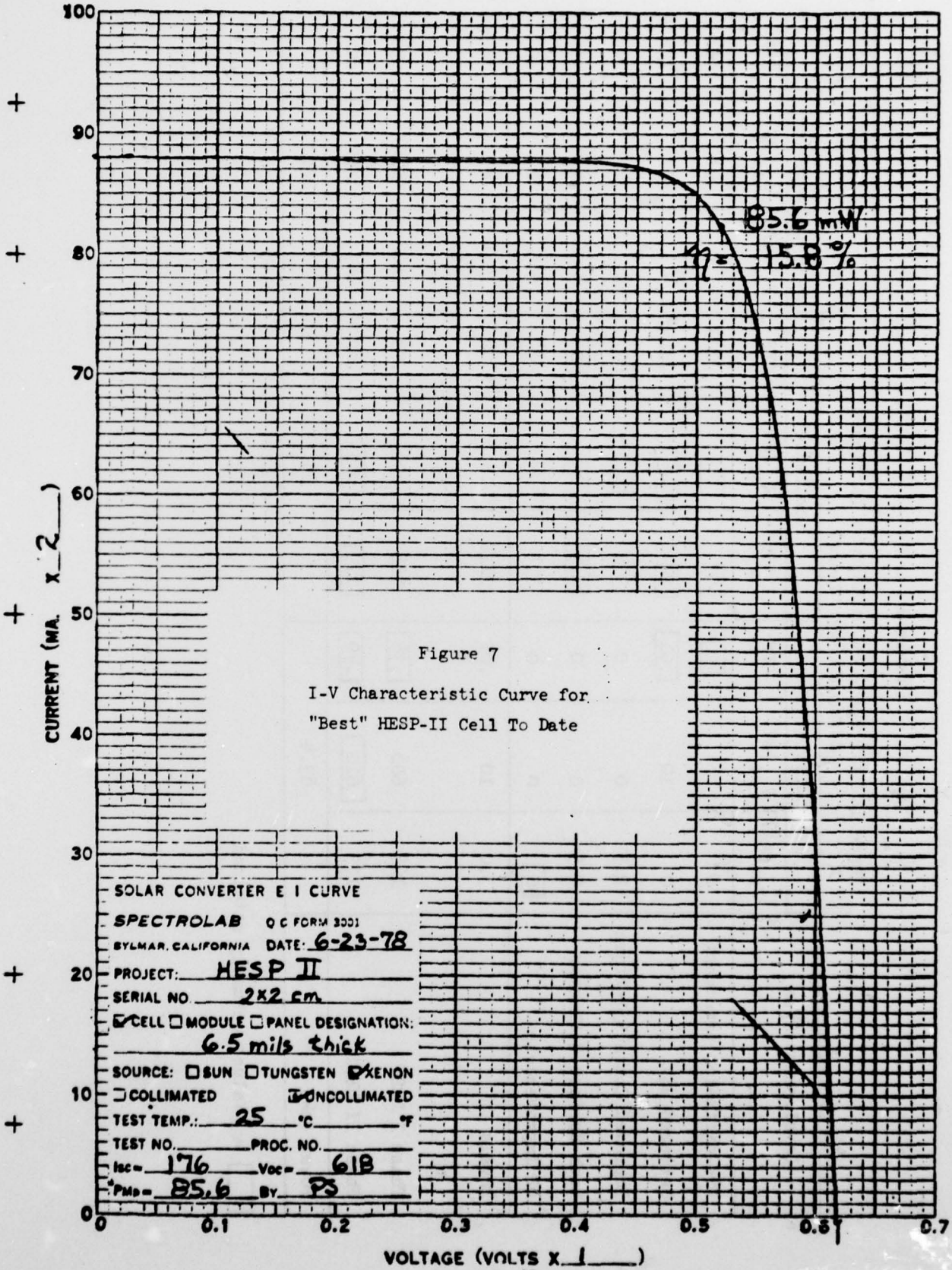

Figure 7

I-V Characteristic Curve for "Best" HESP-II Cell To Date

Table 9

Phase II HESP 2 X 2 cm Cell Power (Achieved) (Without Cover Glass)									
Development Area	Pessimistic			Realistic			Optimistic		
	I_{sc}(mA)	V_{oc}(mV)	CFF	I_{sc}(mA)	V_{oc}(mV)	CFF	I_{sc}(mA)	V_{oc}(mV)	CFF
Pre-diffusion treatment	0	0	[0]	[0]	[0]	.005	1.0	5	.01
Gettered BSF	0	10	[.01]	[2]	[15]	.015	4	20	.02
Improved Contact Pattern	2.5	0	0	[4]	[0]	[0]	5	0	0
Back Surface Reflector	2.5	0	0	[3.5]	[0]	[0]	4.5	0	0
AR Improvements	[0]	0	0	1.5	[0]	[0]	2.5	0	0
Totals	5.0	10	.01	11.0	15	.02	17.0	25	.03
+									
Phase I HESP	168	600	[.78]	168	600	.78	168	600	.78
Phase II HESP	173	[610]	[.79]	[179]	[615]	.80	185	625	.81
Power (mW)		83.4			88.1			93.7	

[ ] = Values actually attained

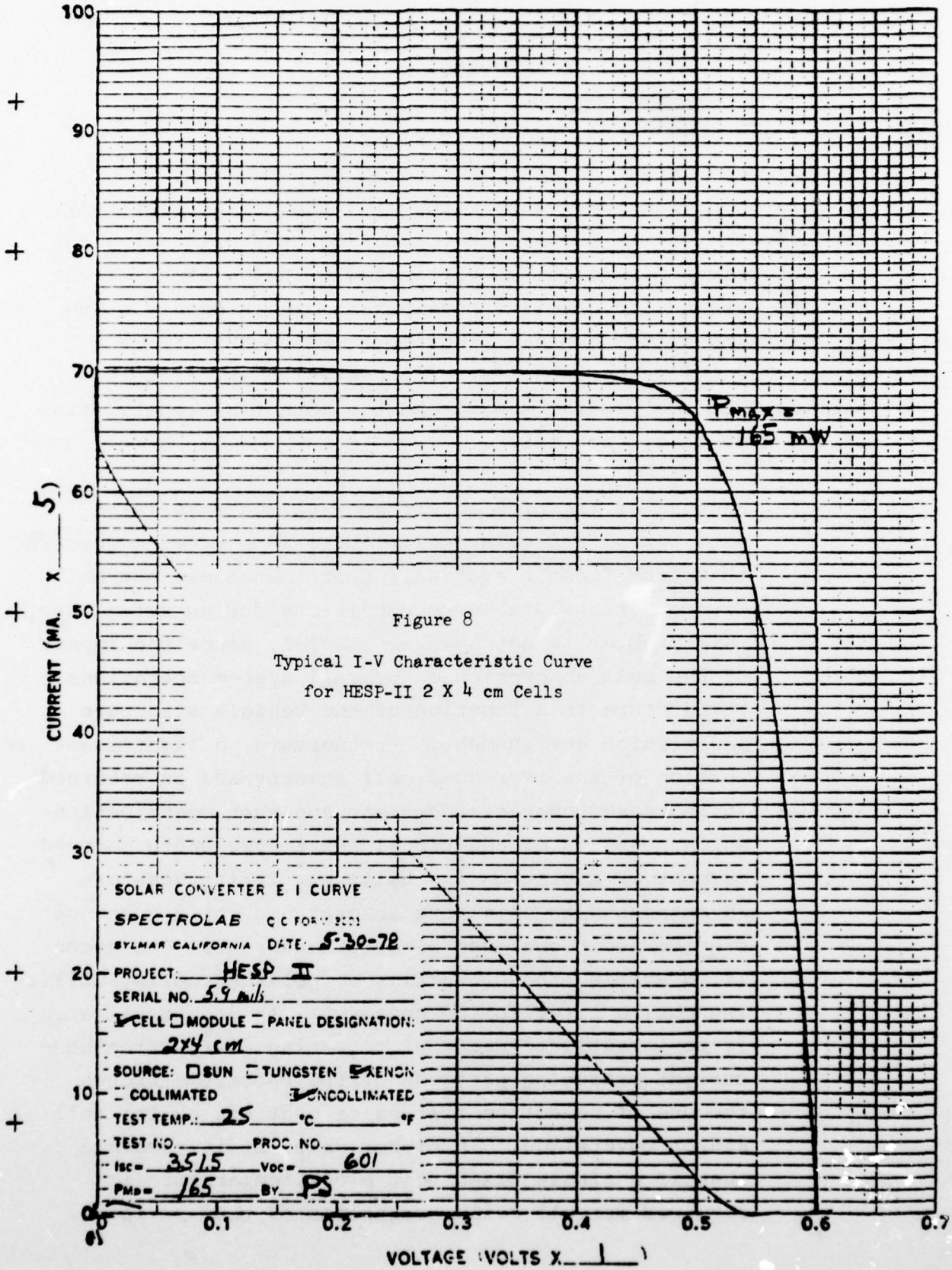

Figure 8

Typical I-V Characteristic Curve
for HESP-II 2 X 4 cm Cells

SECTION IV

RECOMMENDATIONS

At this point in time, roughly the mid-point of a relatively long program, it is worthwhile to consider the original plans and objectives for validity, particularly in the light of the results obtained to date and possible shifts in emphasis and the planning of the overall programs of which HESP-II is a part. The following is a list of items which appear to be pertinent to the program and extend the potential capabilities of the HESP-II silicon cells.

1) Because of the high absorptance values associated with texturized solar cells there is a growing concern that high "test stand" cell performance may not be directly translatable to conditions during actual use. This problem is not however trivial, since the impact of the cell absorption on overall system operational temperature is a function of the vehicle structure and mission environment. Furthermore, a significant portion of the increased cell absorptance is returned as increased operating current and that contribution which consists of additional short wavelength derived current is radiation insensitive. It is therefore advantageous to eliminate absorptance which does not provide additional useful output current. One means is to examine the properties of polished cells, utilizing dual antireflection coatings. An additional area is to investigate means of rejecting energy from non-current producing portions of the spectrum through the use of selective filters or coatings on the cell and/or coverslide. In either case, it is possible that if a single fixed test block temperature is required for all cells, regardles of the α/ε ratio,

then power objectives should be modified accordingly to reflect the different operating temperatures attained on mission.

2) As soon as available, high purity silicon should be investigated for possible use in the HESP program. This would require some adjustment of the processing as well, since the present orientation of the high minority carrier lifetime material is <111> instead of <100> , and this will compromise the back surface field process and texturizing.

3) The effects of cover glassing on HESP-II cell power output should be investigated in order to obtain quantitative data to assist in the design of cell assemblies.

4) State-of-the-art HESP cells should be given electron irradiation screening tests along with gettered sample cells, and float zone material cells, in order to determine potential for meeting contractual EOL goals.

5) The paste process for obtaining back surface field structures should be optimized still further for obtaining higher I_{sc} and V_{oc} values.

6) The use of roughened bottom surface coverglass should be investigated to determine whether girdline reflection loss could be reduced.

REFERENCES

1) "Development of Processing Procedures for Advanced Silicon Solar Cells," NASA CR-134740, January 1975.

2) Hovel, H. J., "Solar Cells," Semiconductor and Semimetals Vol. II, Academic Press, 1975.

3) "High Efficiency Solar Panel (HESP)", AFAPL-TR-77-36, 1 July 1977.

4) Fossum, J. G., "Computer Aided Numerical Analysis of Silicon Solar Cells," Solid State Electronics, Vol. 19, p. 269, 1976.

5) Lindholm, F. A., and Sah, C. T., "Fundamental Electronic Mechanisms Limiting the Performance of Solar Cells," IEEE Transactions on Electron Devices, ED-24 No. 4, p. 299, UPI April 1977.

6) Private Communication, Dr. Sprygada.

*U.S.Government Printing Office: 1979 — 657-002/416